SUM4Re

Creating materials banks
from digital urban mining

D2.3: XRF methodological framework acquisition

VERSION 1.0

28 October 2025

PUBLIC

Associated with document Ref. 101129961

Funded by the European Union. Views and opinions expressed are however those of the author(s) only and do not necessarily reflect those of the European Union. Neither the European Union nor the granting authority can be held responsible for them.

Funded by the European Union

SUM4Re

Creating materials banks from digital urban mining

Deliverable ID	D2.3
Deliverable name	XRF methodological framework acquisition
Lead partner	OLAR
Contributors	MOYUA

PUBLIC

Funded by the European Union

DOCUMENT INFORMATION

Document name	D2.3 XRF methodological framework acquisition
Version	1.0
Due date	31/10/2025
Report date	28/10/2025
Number of pages	55
Lead Author	Pablo José Arauzo Gimeno (OLAR)
Other Authors	Maciej Pawel Olszewski (OLAR)
Dissemination level	Public

REVISION HISTORY

Rev.	Date	Description of revision
0.1	30/09/2025	Initial version
0.2	21/10/2025	Revised draft
1.0	28/10/2025	Final version (approved)

DOCUMENT APPROVAL

Written	Pablo José Arauzo Gimeno (OLAR) Maciej Pawel Olszewski (OLAR)	30/09/2025
Revised	Ourania Patsia (EAGLE)	09/10/2025
	Ana Sánchez (UVIGO, Project Manager)	28/10/2025
Approved	Pedro Arias Sánchez (UVIGO, Project Coordinator)	28/10/2025

EXECUTIVE SUMMARY

Deliverable D2.3 (Task 2.3) reports on the development, validation and integration of a novel analytical and computational framework for identifying construction and demolition materials and includes the X-ray Fluorescence (XRF) methodological framework, its limitations and AI model specifications, as well as a material library. This work is fundamental to work package (WP) 2, as it establishes the datasets and protocols necessary for subsequent AI modelling (WP3), and pilot demonstrations (WP10).

The initial phase of the project involved preparatory activities such as calibrating analytical instruments, developing standardised sampling procedures, and collaborating with the Spanish pilot sites (Anoeta Station and the OTIS factory in San Sebastián). Representative materials, including concrete and asphalt, were collected, dried and homogenised to ensure reproducibility. Portable XRF (p-XRF) (Oxford X-MET 7500) was used for rapid screening in situ, while laboratory XRF (Malvern Panalytical Epsilon 1) was used to make high-quality reference measurements. Complementary analyses were performed using inductively coupled plasma optical emission spectroscopy (ICP-OES) (Thermo Fisher iCAP 7200 Duo), following microwave digestion with a Milestone ETHOS EASY, and X-ray Diffraction (XRD) (Bruker D2 Phaser). This enabled the quantification of elements in bulk and the identification of mineralogical phases.

The second phase consisted of a sampling and acquisition campaign which produced a dataset of 29 p-XRF measurements distributed across the pilot sites. This was combined with laboratory analyses of three concrete samples and one asphalt sample. All measurements were performed under strict quality assurance protocols, including the use of certified reference materials (CRMs), triplicate analyses and continuous instrument stability checks. The figures and tables in this deliverable illustrate the composition of the dataset, the distribution of the measurement points and the reproducibility metrics.

The third phase focused on developing machine learning regression models. Several algorithms were benchmarked using the integrated dataset, laboratory ICP-OES references and XRD descriptors. Random forest regression (RFR) and artificial neural networks (ANN) produced the most accurate results, achieving R^2 values above 0.90 for major oxides and trace elements. The models successfully distinguished between concrete, asphalt and masonry fractions with 96% accuracy in classification, while also identifying hazardous thresholds (e.g., Pb >0.01%, Cr >0.02%), in accordance with the requirements of the European Union (EU) waste framework directive.

Despite these achievements, the deliverable acknowledges technical and methodological constraints. XRF remains surface-sensitive and susceptible to matrix effects; ICP-OES necessitates intricate digestion protocols; and XRD is limited in its ability to detect amorphous phases. Methodologically, dataset size and representativeness are the main bottlenecks, particularly for trace metals. Overfitting risks in neural networks and limited uncertainty quantification were also identified as challenges. Section 5 details these constraints and outlines mitigation strategies, including expanded sampling, improved calibration routines and the integration of mineralogical descriptors into ML models.

GLOSSARY

Terms, Abbreviations, and Acronyms

XRF	X-ray Fluorescence
WDXRF	Wavelength-Dispersive X-ray Fluorescence
EDXRF	Energy-Dispersive X-ray Fluorescence
SDD	Silicon Drift Detector
p-XRF	Portable X-ray Fluorescence
CDW	Construction and Demolition Waste
CRMs	Certified Reference Materials
SOP	Standard Operating Procedure
EPA	Environmental Protection Agency
ICP-OES	Inductively Coupled Plasma Optical Emission Spectrometry
WP	Work Package
AI	Artificial Intelligence
ML	Machine Learning
ANN	Artificial Neural Network
SVR	Support Vector Regression
RFR	Random Forest Regression
PLSR	Partial Least Squares Regression
BIM	Building Information Modelling
C-BIM	Circular Building Information Modelling
GENIA	Platform for Structural Model Generation
DBL	Digital Building Logbook
DPP	Digital Product Passport
GDPR	General Data Protection Regulation
NIST	National Institute of Standards and Technology
REACH	Registration, Evaluation, Authorisation and Restriction of Chemicals
CLP	Classification, Labelling and Packaging Regulation
CE	Conformité Européenne (European Conformity)
ISO/IEC	International Organization for Standardization / International Electrotechnical Commission

ICDD	International Centre for Diffraction Data
FP	Fundamental Parameters
ISDS	Intelligent Scientific Data Solution
EU	European Union
EWC	EU Waste Catalogue
XRD	X-ray diffraction

TABLE OF CONTENTS

LIST OF TABLES

LIST OF FIGURES

1. Introduction

1.1. SUM4Re research context and approach

The SUM4Re project ("Creating material banks from digital urban mining") is a European initiative funded by Horizon Europe (ID 101129961), running from June 2024 to November 2027. Its main goal is to turn construction and demolition waste—the largest waste stream in the EU—into reusable "material banks." This is achieved by combining urban mining (selective reuse), advanced technologies (automated scanning, AI, circular BIM, blockchain), and a systematic approach to identifying, analysing, and tracking materials. Three pilot projects will be carried out in Spain, the Netherlands, and Norway. The project brings together 17 partners, including universities (coordinated by the University of Vigo), technology centres, and companies in the construction and digitalization sectors. The ultimate objective is to boost circularity in construction through digital tools and open standards—reducing waste, increasing the supply of secondary raw materials, and fostering new business models based on the circular economy.

1.2. Scope and purpose of deliverable D2.3

This delivery service serves to describe the progress made and results achieved for Task 2.3:

T2.3. Data collection for identification of materials & construction products with XRF (M3-M17) OLAR; MOYUA

The aim of this task is to build an extensive library of construction materials using XRF [OLAR]. To enable real-time identification of construction materials and products on-site, AI algorithms trained with a thorough database are required. ICP combined with Optical Emission Spectroscopy (ICP-OES), is widely used for comprehensive elemental analysis, and can detect major and trace elements (composition information). The ICP analysis is done only in liquid phase, so it is necessary to prepare the solid samples by microwave digestion. The following steps will be conducted: (1) Establishment of a data collection process by using XRF for raw and constructed materials. (2) Acquisition of a large collection of samples XRF, comprising the main construction materials for the demonstrators (concrete & asphalt). (3) Samples characterization with ICP-OES for reference detailed composition (4) Development of ML regression models for material identification. The best performing models for material identification will be applied to the demonstrators in WP10 in collaboration with MOYUA.

2. Research approach

2.1. State of the art

X-ray fluorescence (XRF) is a well-established technique that can be used to analyse the elements of solids, powders and liquids without destroying them. The signal is created when X-rays are released from the atom and the atom relaxes by emitting lines of light. The energy of these lines tells us what the elements are and how strong the lines are. This can be measured accurately. Two types of instruments stand out: wavelength-dispersive XRF (WDXRF), which uses crystals to separate lines to achieve high spectral resolution, and energy-dispersive XRF (EDXRF), which measures photon energies directly with silicon drift detectors (SDDs). The basics of this and how instruments are used are clearly explained in many books and technical reports (Brouwer 2010).

For materials used in construction (like concrete, asphalt, aggregates, cements, and metals), portable XRF (p-XRF) is an effective tool for quickly testing and sorting materials at the site of their use. Recent studies have shown that p-XRF can accurately measure heavier oxides and important alloying elements when surfaces are prepared correctly and the right calibrations are used. This was applied for some elements that can be difficult to measure (e.g., Al and Si) and for different types of binders, which are common in construction and demolition waste (CDW) streams (Zhen L. 2024).

At the same time, guidance documents (e.g., United States Environmental Protection Agency, US EPA Method 6200 (U.S. Environmental Protection Agency 2007)and field standard operating procedure, SOPs (U.S. Environmental Protection Agency. 2023, 2024)) set out the best ways to do this: controlling moisture/thickness, taking multiple shots and using certified reference materials (CRMs), and deciding when to collect samples for testing in a lab. These standards are widely used for soil and solids and can be used directly for building materials surveys.

The measurements using p-XRF are very fast (few seconds to few minutes) and can be used many times without damaging the sample, but it is sensitive to the surface (i.e., it can provide information about depths from tens of micrometres to sub-millimetres, depending on the element and the material it is analysed in) and the effect of the material on the result can vary depending on the material. So, it is very important to calibrate the results according to the material and the environment, and to regularly check the results in a laboratory. This is necessary to make sure that the results can be used for compliance or material passporting. The instructions for doing experiments and the manuals for the labs all agree on these physical limits, and on the need for the samples to be prepared properly (e.g., cleaned, smoothed, or melted down for further analysis) (Brouwer 2010).

Inductively coupled plasma optical emission spectrometry (ICP-OES) is a laboratory method where the solid sample (after being digested or dissolved) is sprayed into a stream of argon gas; the excited atoms/ions give off light at specific wavelengths that are spread out and measured using a spectroscope. ICP-OES can measure multiple elements, has a wide range of linear dynamic range, and can detect elements at lower levels than XRF for many elements. It uses standard methods for environmental and solid-waste samples (e.g., EPA 6010D). Modern instruments (axial/radial or duo view) can detect very low levels (i.e., in the range of milligrams per kilogram) in normal set-ups, and there are tables that show the lowest levels that can be detected for common substances (Thermo Fisher Scientific 2025).

In cementitious and mineral materials, ICP-OES is widely used as the bulk-truth technique because digestion makes all the different parts (i.e., binder, aggregate and coatings) the same sample. Comparative studies in binders and cements show that ICP-OES and XRF can agree extremely well for major oxides when the right calibrations and preparations are used, but ICP-OES is better for measuring very small amounts and for elements where XRF sensitivity or spectral overlaps are limiting. Many scientific papers in the fields of cement chemistry and

analytical science show this similarity and have confirmed that EDXRF methods are as good as ICP-OES for binder chemistry when fused-disk or pellet protocols are followed (Marjanovic et al. 2000; Mijatović et al. 2019).

Currently, the best practise that highly relevant to Task 2.3 (M3–M17), is to combine p-XRF screening on-site with periodic ICP-OES laboratory anchoring on representative micro-samples. This hybrid approach: use p-XRF to map variability quickly, then select a subset for laboratory digestion and ICP-OES to (i) establish/refresh calibration curves, (ii) quantify elements at or near threshold limits, and (iii) verify heterogeneous or borderline cases.

2.2. Relevance to the WP2 objectives

The state of the art in XRF and ICP-OES technologies support the goals of WP2, which aims to create a strong set of methods for identifying and describing materials in construction and demolition situations. WP2's objectives are to study geometrical, radiometric, logistical, and temporal condition factors for fast, safe, and efficient data acquisition for each demonstrator. Based on the identified factors, the most adequate equipment will be chosen, the acquisition had been planned, and the data obtained had been prepared for further processing.

Task 2.3 makes sure that WP2 creates a scientifically proven way of doing things. It does this by combining the advantages of p-XRF (i.e. rapid scanning, testing in a non-destructive manner and ability to perform multiple tests fast) and ICP-OES (i.e., being very precise, and able to spot very small amounts). This mixed approach is very important for dealing with the variety of construction and demolition waste: XRF provides fast screening on-site, while ICP-OES provides precise calibration and accuracy at very low levels. Together, they help to create the information that is needed to train AI models (WP3) that can accurately predict the composition of large groups of things from surface measurements.

Moreover, if we make sure that the XRF and ICP-OES methods match up with the WP2 goals, it will create a trustable and accurate library of reference materials. The library will contain paired datasets that document both surface and bulk chemical signatures across representative construction products (i.e., concrete, asphalt,). This data is very important for creating models that can predict future outcomes, and for making sure that digital building logbooks and material passports can be traced, as planned in the project's circular economy strategy.

Finally, the clear understanding of XRF's limits (e.g., sensitivity to surface effects, problems with mixtures of elements, and reduced sensitivity to light elements) and the use of ICP-OES to correct problems addresses WP2's focus on quality control and standardisation. The two methods are used together.

2.3. Relevance to the other WP objectives

Task 2.3 focuses on the systematic acquisition of elemental composition data for representative construction materials and products using portable p-XRF. The aim is to build a reference material library and it is mainly related to:

- WP3. Specifically, the Task 3.3. Material properties prediction with XRF focuses on the development and optimization of artificial intelligence (AI) models (machine learning, ML regression) to quantify specific properties of interest regarding construction materials (i.e., concrete and asphalt). Task 3.7. Data upload to Platform for Structural Model Generation (GENIA) for C-BIM structural model generation, wherein different intelligent solutions including XRF are used to quick digitalize the built environment focused on structural components will be researched and implemented.
- WP10. The use of the XRF technology is used for concrete and asphalt characterization.

2.4. Legal considerations

The utilization of XRF and ICP-OES in construction and demolition environments must be aligned with both instrument-specific regulations and sector-specific legal frameworks.

2.4.1. Instrument safety and certification.

XRF uses ionising radiation, which means handheld and portable devices must follow EU radiation safety rules (e.g., Council Directive 2013/59/Euratom, Basic Safety Standards). Manufacturers must provide CE-marked instruments that meet the ISO/IEC 61010 standards for electrical safety and the ISO 13181/ISO 3497 standards for XRF methodology. Operators must have training that is documented and that covers safe use, shielding, and storage. This is even though modern portable XRFs use low-power X-ray tubes and are generally not subject to heavy licensing in most EU Member States. ICP-OES, on the other hand, does not use ionising radiation. Instead, it follows safety rules for using pressurised gases, high-frequency power supplies and acid digestion (e.g., Registration, Evaluation, Authorisation and Restriction of Chemicals (REACH)/ Classification, Labelling and Packaging Regulation (CLP) for chemicals used in sample preparation).

2.4.2. Environmental and waste regulation compliance.

When it is used to characterize construction and demolition waste (CDW), both XRF and ICP-OES outputs comply with EU legal frameworks such as the Waste Framework Directive (2008/98/EC, amended 2018/851) and the Construction Products Regulation (EU No 305/2011). XRF can quickly check that materials that are going to be reused or recycled do not have too many hazardous substances (e.g., Pb, Cd, Cr(VI)). ICP-OES validation makes sure that the concentrations of these substances do not go beyond the legal limits. When the EU Waste Catalogue (EWC) codes are used in a country, it is important to know what the waste actually is, so that the right code can be used. ICP-OES is often the method that is used to figure out what the waste is made of.

2.4.3. Worker health, safety, and liability.

The information produced by XRF and ICP-OES can directly affect decisions about how much workers are exposed to risk and who is responsible for it in demolition projects. For example, XRF-based detection of Pb in coatings or Cr in cement triggers legal obligations under Directive 2004/37/EC (Carcinogens and Mutagens at Work Directive) and Directive 98/24/EC (Chemical Agents Directive). Employers must do risk assessments and take safety measures if they spot dangerous levels. This makes it important to check that the data is reliable and can be traced. While no specific radiation protection equipment is required for the operation of portable X-ray fluorescence devices, the use of a sample stand and comprehensive operator training is essential, with the optional use of gloves and safety glasses depending on the characteristics of the material under investigation.

2.4.4. Data traceability and standardisation.

From a legal and standardisation point of view, the results of an analysis must be able to be traced back to the original sample, able to be reproduced, and defendable. ICP-OES is used in a lot of ISO and EN standards for construction and environmental materials (e.g., EN 196-2 for analysing cement). XRF is mentioned more and more in technical guides (e.g., US EPA Method 6200 for field p-XRF, with similar European methods under CEN/TC 351 and CEN/TC 444). To be included in Digital Product Passports (DPPs) and Digital Building Logbooks (DBLs), it is necessary to comply with EU data governance rules (e.g., Regulation (EU) 2022/868 on European data governance).

2.4.5. Privacy and contractual aspects.

In renovation and demolition projects, information about chemicals in buildings may be considered private business information, particularly if it affects responsibility or the value of the building. So, contracts with building owners and contractors must include information about

who owns the data, how it can be used, and how it must be kept secret. The General Data Protection Regulation (GDPR) does not apply directly to basic data, but metadata about a project (e.g., geolocation, building owner identity) must be handled in accordance with data protection rules.

2.5. Target materials

The XRF methodological framework (Task 2.3) is designed to cover the most common construction and demolition materials in European buildings. These materials are important for assessing how well the circular economy works, identifying hazards, and creating material passports.

Concrete is the biggest part of CDW by mass. XRF is good at detecting major oxides (e.g., Si, Ca, Al, Fe) and trace contaminants (e.g., Pb, Cr, Zn), while ICP-OES validation makes sure that binders and aggregates are characterised accurately. We pay extra attention to the layers of carbonation and surface coatings, where heavy metals can build up.

Asphalt pavements are another type of waste that is produced in large quantities. XRF can identify mineral filler composition (e.g., Ca, Si, Al) and detect hazardous additives such as heavy metals (e.g., V, Ni from bitumen, Pb from historical pigments). ICP-OES validation is a way to accurately measure trace metals to meet regulatory compliance requirements.

2.6. Case studies application

The Spanish pilot site consists of two buildings in San Sebastián (Figure 1 and Figure 2). These buildings show different situations where the XRF methodological framework under Task 2.3 can be used. These pilots show a public building that is being rebuilt (Anoeta station) and an old industrial site (Jolastokieta) that has been left for being converted into a residential location. This means that they include different materials and situations where buildings are being rebuilt or destroyed.

The Anoeta station is a public train station undergoing remodelling, which makes it an ideal environment to test the practical application of the XRF methodological framework in both open and confined construction contexts. By applying XRF systematically to the Anoeta Station, the project will generate asphalt data.

Figure 1. Spanish case study (Anoeta Station)

The second building is an abandoned industrial factory in Jolastokieta. The site is largely empty, with only the structural framework remaining. Thin metal beams and columns once used to support heavy machinery are still present, while the floor, ceiling, and walls are composed of stone, metal, and concrete, respectively. This site provides a contrasting scenario, where XRF can be applied to characterize aged, weathered materials in a derelict industrial environment. An interior view is shown in Figure 2, and additional details are provided in Deliverable D10.1.

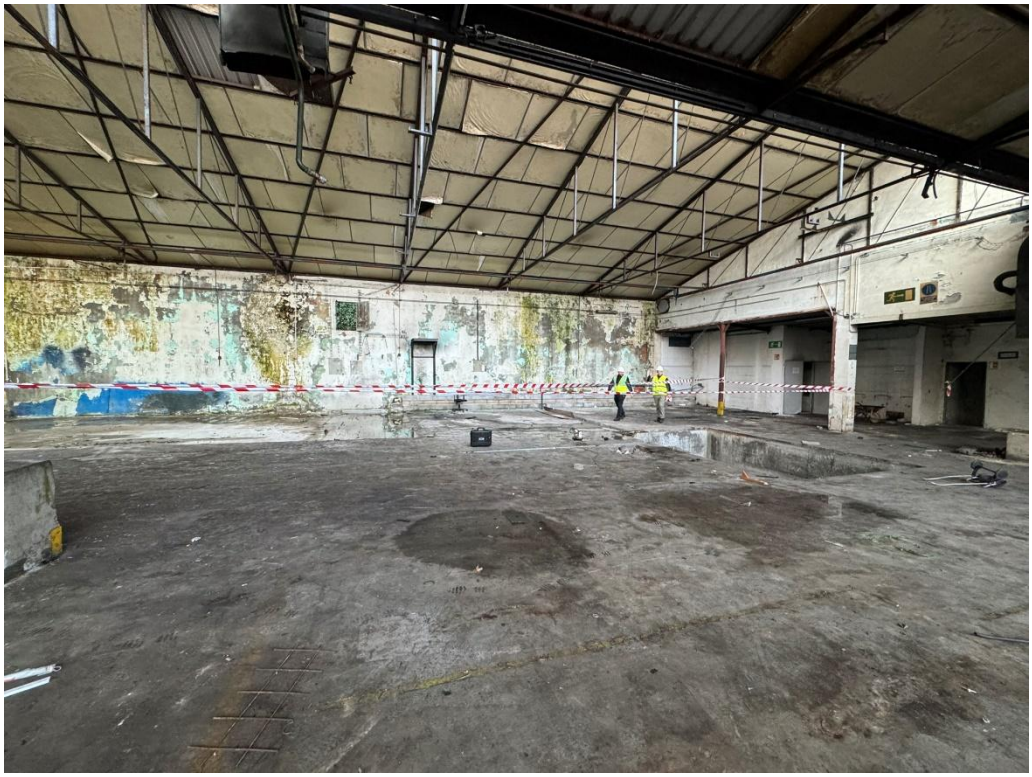

Figure 2. Spanish case study (Jolastokieta)

3. Technical brief

To determine the inorganic composition of representative construction and demolition material samples, a multi-instrumental analytical workflow was implemented, combining p-XRF and ICP-OES. Additionally, lab-bench X-ray fluorescence (EDXRF) and X-ray diffraction (XRD) were utilized. This approach ensures complementary insights: XRF for rapid non-destructive screening, ICP-OES for trace-level, bulk-accurate quantification, and XRD for crystalline phase identification.

On-site measurements were carried out with an Oxford Instruments X-MET 7500 handheld spectrometer, featuring a Rh anode X-ray tube, a high-resolution SDD, and an automatic 5-position filter changer that allows optimized excitation for different groups of elements. Like the laboratory instrument, quantification was based on the SOILS-LE FP calibration, ensuring methodological consistency across datasets. The portable format enables rapid in situ elemental screening, critical for demolition and renovation surveys where speed and non-destructiveness are key. Each measurement consisted of a 60-second live-time acquisition, covering elements from magnesium (Mg) to uranium (U). Moreover, to ensure the data reliability, the following approaches were applied: 1) CRMs (BCR-032 #919 and GMB306-12) were pressed into 32-mm pellets and analysed at the beginning and end of each measurement run. 2) Instrument stability was verified through periodic recalibration and background checks.

To obtain bulk-accurate elemental concentrations, representative samples were digested and analyzed using an iCAP 7200 ICP-OES Duo (Thermo Fisher Scientific). Sample preparation was performed with a microwave digestion system ETHOS EASY (Milestone), which enables efficient dissolution of complex matrices, such as silicate-rich and carbonate-rich concretes. ICP-OES offers superior sensitivity than XRF and multi-element capability, with detection limits in the low $mg \cdot kg^{-1}$ range, providing a benchmark for validating XRF results and for quantifying elements that are challenging for XRF due to spectral overlaps or poor light-element sensitivity.

Laboratory XRF analyses were performed using a Malvern Panalytical Epsilon 1 spectrometer equipped with a Rhodium (Rh) X-ray tube and a high-resolution (SDD). Quantification employed the SOILS-LE calibration program with the fundamental parameters (FP) method to correct for matrix effects.

To complement elemental analysis, crystalline phases in the concrete samples were identified utilizing a Bruker D2 Phaser 2nd Gen equipped with a radiation source Cu Kα (1.5406 Å), a LYNXEYE-2 position-sensitive detector. Phase identification was performed by diffraction pattern matching against the International Centre for Diffraction Data (ICDD) database, enabling detailed characterization of cement hydrates, aggregates, and alteration products. This mineralogical information provides critical context for interpreting XRF and ICP-OES results, especially in heterogeneous materials such as concrete and stone.

3.1. Equipment technical specification

The technical characteristics of the different analytical equipment is shown in Table 1.

Table 1. Technical specification of different analytical techniques used in the T2.3

Instrument	Type / Mode	Key Technical Specifications	Element / Phase Range	Role in Task 2.3
Malvern Panalytical Epsilon 1 (EDXRF)	Laboratory, benchtop	Rh anode X-ray tube (50 kV), SDD detector (~135 eV), SOILS-LE FP calibration, 60 s live-time, 32 mm pellets, CRMs used for QC	Mg → U	High-precision lab-based elemental quantification; reference-quality XRF data for calibration and comparison with ICP-OES

Oxford X-MET 7500 (pXRF)	Portable, field-based	Rh anode tube (50 kV, 50 µA), SDD (~145 eV), 5-position automatic filter, rugged IP54, battery ~10 h, GPS-enabled	Mg → U (matrix dependent)	Rapid in situ elemental screening of construction materials; supports non-destructive, georeferenced acquisition in pilot sites
Thermo Fisher iCAP 7200 ICP-OES Duo	Laboratory, bulk analysis	Dual view (axial/radial plasma), 166–847 nm range, low µg·L^{-1} detection limits, argon plasma	Multi-element, trace to major	Bulk-accurate reference quantification; anchors XRF results, especially for trace and light elements
Milestone ETHOS EASY (microwave digestion)	Laboratory, sample prep	High-pressure closed vessels, up to 300 °C and 100 bar, 15 samples/run, real-time T/P control	Enables full digestion of silicates, carbonates, metals	Ensures complete dissolution of concrete and stone matrices for accurate ICP-OES analysis
Bruker D2 Phaser 2nd Gen (XRD)	Laboratory, phase analysis	Cu Kα source (λ = 1.5406 Å, 30 kV/10 mA), LYNXEYE-2 PSD, 2θ range 5–90°, ICDD PDF-2 database	Mineral phases (cement hydrates, aggregates, alteration products)	Identifies crystalline phases; contextualizes XRF/ICP-OES results and builds mineralogical dataset

3.2. Equipment description with respect to application and utilization

To establish a robust methodological framework for the characterization of construction and demolition materials, Task 2.3 employs a combination of laboratory and field instruments. Each piece of equipment provides complementary data that together enable rapid, reliable, and scientifically validated material identification.

3.2.1. p-XRF

Its rugged, battery-powered design allows use in demolition and renovation environments, while integrated GPS enables georeferencing of measurements. In Task 2.3, the X-MET 7500 is utilized for on-site acquisition, supporting rapid non-destructive data collection and contributing directly to the project's material library.

3.2.2. ICP-OES

Samples are prepared through complete microwave digestion to ensure matrix dissolution. The instrument's role in Task 2.3 is to act as the reference technique for calibration and validation of p-XRF data, particularly for elements where p-XRF is less sensitive (e.g., light elements) or where matrix effects introduce bias. This ensures that the material datasets used for AI model development (WP3) are anchored to laboratory-grade accuracy.

3.2.3. EDXRF

It is used in the project for high-precision laboratory measurements of pressed pellet samples. Its application is particularly relevant for the validation of field XRF measurements, as it provides stable and reproducible results across a wide elemental range (Mg–U). The use of CRMs ensures data traceability and quality control. Within Task 2.3, the Epsilon 1 serves as the laboratory XRF benchmark, bridging portable field measurements with ICP-OES bulk analysis.

3.2.4. XRD

Its utilization within Task 2.3 is complementary, whereas XRF and ICP-OES provide elemental concentrations, XRD identifies the mineralogical phases present (e.g., portlandite, calcite, quartz, feldspar, hydrates). This enables a more comprehensive characterization of material properties and provides critical context for interpreting compositional data.

3.3. Preparatory measures

Several preparatory measures were undertaken before initiating systematic data acquisition with XRF and ICP-OES to ensure the reliability, efficiency, and reproducibility of the results. These measures covered sample selection and handling, device calibration, and logistical coordination with the pilot sites.

First, both the XRF spectrometers and the ICP-OES were calibrated. OLAR carried out the calibration to guarantee the accuracy and comparability of the results obtained from field p-XRF and laboratory (EDXRF, ICP-OES) measurements. Regular recalibration and the use of CRMs were integrated into the preparatory workflow to monitor instrument stability.

Sample collection was identified as a key parameter for WP2. In collaboration with MOYUA, representative materials were selected at the pilot sites to minimize interferences such as humidity or heterogeneity. Specifically, one asphalt sample was collected from the Anoeta Station, and two concrete samples were collected from the Jolastokieta industrial site. To ensure standardized treatment, sampling protocols were defined for both on-site XRF measurements and laboratory analyses at OLAR. Once received, the samples underwent preliminary processing, including drying, sieving, and grinding. They were then transferred into sealed containers to prevent contamination or degradation prior to analysis (Figure 3).

Figure 3. Samples collected by MOYUA prior XRF and ICP-OES analysis by OLAR

In parallel, preparatory visits and agendas were organized with MOYUA to coordinate access to the sites and sampling schedules at the pilot units. This included defining sampling dates, securing the necessary permits, arranging accommodation for field teams, and developing agendas that minimized disruption to ongoing work at construction and demolition sites.

These preparatory measures ensured that Task 2.3 could begin data acquisition using a standardized, reproducible approach while maintaining strong collaboration between OLAR and MOYUA. The preparatory phase established the baseline for subsequent large-scale XRF acquisition, laboratory validation, and integration of the results into the project's material library.

3.4. Sampling methods

The design of the sampling methodology in Task 2.3 was guided by three principles: representativeness, reproducibility and traceability. As the objective of this task is to establish

a robust methodological framework for the XRF-based identification of construction materials, which is subsequently validated using ICP-OES and XRD, the acquisition strategy had to bridge the gap between rapid, non-destructive, in situ screening and bulk-sensitive laboratory analyses.

3.4.1. Time allocations

Fieldwork at the MOYUA demonstrators in San Sebastián (Anoeta Stadium and the OTIS factory) was planned to strike the right balance between speed and data quality. Each portable XRF measurement was configured for a 60-second acquisition time, chosen to allow the detection of both major and trace elements while minimising operator fatigue and time constraints. However, the actual time taken for each measurement was longer, typically 2–3 minutes, once surface preparation, instrument positioning, stabilisation and metadata recording were taken into account.

During the April 2025 campaign, a total of 29 valid measurements were performed across six distinct zones in a single working day. This confirmed the practical throughput of 40–60 measurements per hour per operator, which was consistent with expectations and the instrument's technical specifications. Table 2 of the report presents the distribution of these measurements, detailing their allocation across structural elements at the OTIS factory and the asphalt section of Anoeta Stadium.

Laboratory work was more time-intensive. Bulk samples collected on site were dried at a controlled temperature, ground and sieved to ensure homogeneity of particle size prior to analysis. Preparing pressed pellets for EDXRF analysis took an extra 2–3 working days, including batching, equipment calibration, and quality control. XRD analyses were performed on powdered samples, with each scan covering the 2θ range from 5° to 90° and taking approximately 20–30 minutes per sample. Using the Bruker D2 Phaser enabled relatively fast throughput while maintaining high resolution.

ICP-OES analysis, by contrast, involved more extended time allocations. Each digestion batch using the ETHOS EASY microwave system took between 4 and 6 hours, with a batch capacity of 15 vessels. The subsequent ICP-OES runs on the Thermo Fisher iCAP 7200 Duo required one working day for calibration with multi-element standards, optimization of axial/radial plasma views, and analysis of the digested solutions. Because concrete samples present a particularly complex silicate-carbonate matrix, this step was scheduled after the initial XRF and XRD analyses, enabling the digestion protocol to be optimized according to preliminary findings.

Table 2. presents the elemental composition of the 29 spots analyzed during the in-situ measurements (detailed spectra are provided in Appendix Figure. A1). The results approach 100% in total elemental weight (%).

Sample location	Inorganic compound (wt.%)												
	Mg	Al	Si	P	S	Cl	K	Ca	Ti	V	Cr	Mn	Fe
otis-I.1	0.0 ± 0.0	2.9256 ± 0.1567	3.0369 ± 0.0621	0.5815 ± 0.0195	9.3693 ± 0.0418	1.5559 ± 0.0174	30.3782 ± 0.0761	47.6488 ± 0.1018	0.2133 ± 0.0098	ULLD	0.065 ± 0.0164	0.0667 ± 0.0142	3.2238 ± 0.0358
otis-I.1.humedo	0.0 ± 0.0	1.785 ± 0.1387	1.0802 ± 0.0418	0.5685 ± 0.018	16.474 ± 0.0514	1.6377 ± 0.0176	44.1078 ± 0.0913	30.8616 ± 0.0875	0.1143 ± 0.0084	ULLD	0.0403 ± 0.0134	0.0622 ± 0.0123	2.3833 ± 0.0291
otis-I.2	3.0332 ± 0.8049	2.8271 ± 0.1463	3.2041 ± 0.0614	0.6741 ± 0.0185	0.9468 ± 0.0136	1.3534 ± 0.0145	6.1036 ± 0.0303	76.6337 ± 0.0978	0.3115 ± 0.0103	ULLD	0.0486 ± 0.0155	0.0903 ± 0.0148	3.686 ± 0.0377
otis-I.3	0.0 ± 0.0	3.1411 ± 0.1551	4.0997 ± 0.0684	0.6517 ± 0.0191	3.4948 ± 0.0254	1.4108 ± 0.0152	11.4654 ± 0.0426	70.1804 ± 0.0978	0.3349 ± 0.0106	ULLD	0.0568 ± 0.0156	0.0939 ± 0.0149	4.0095 ± 0.039
otis-I.4	0.0 ± 87.7689	2.1994 ± 0.1539	3.4065 ± 0.0649	0.6007 ± 0.0197	0.6861 ± 0.0123	1.4239 ± 0.0149	4.1739 ± 0.0248	82.1692 ± 0.0988	0.3128 ± 0.0104	ULLD	ULLD	0.1293 ± 0.0134	3.7139 ± 0.0381
otis-I.5	0.0 ± 0.0	2.0379 ± 0.1603	2.8508 ± 0.0627	0.5443 ± 0.02	0.935 ± 0.0144	1.2124 ± 0.0144	5.5871 ± 0.0291	81.0928 ± 0.1003	0.315 ± 0.0106	ULLD	0.0688 ± 0.017	0.1054 ± 0.016	4.0422 ± 0.04
otis-II.1	0.0 ± 0.0	1.8105 ± 0.2725	2.4104 ± 0.0973	1.2568 ± 0.0432	20.0433 ± 0.0929	4.0669 ± 0.0457	1.2308 ± 0.0291	64.0763 ± 0.1421	0.214 ± 0.0176	ULLD	0.1805 ± 0.0341	ULLD	4.1862 ± 0.06
otis-II.2	0.0 ± 0.0	1.9287 ± 0.2086	2.1532 ± 0.0725	0.8462 ± 0.0285	21.8943 ± 0.0811	3.3963 ± 0.0343	1.0743 ± 0.0203	64.8307 ± 0.1206	0.1167 ± 0.0132	ULLD	0.0698 ± 0.0231	ULLD	2.9334 ± 0.043
otis-II.3	0.0 ± 0.0	3.7172 ± 0.245	12.2794 ± 0.1531	0.9229 ± 0.0355	2.8009 ± 0.0331	7.6874 ± 0.0488	3.6242 ± 0.0353	58.2515 ± 0.1124	0.7618 ± 0.017	ULLD	0.0925 ± 0.0246	0.1115 ± 0.0217	9.0003 ± 0.0716
otis-II.4	0.0 ± 0.0	2.4282 ± 0.2147	4.4283 ± 0.091	0.8287 ± 0.0276	12.8429 ± 0.0598	4.1378 ± 0.034	2.0152 ± 0.0241	67.3985 ± 0.1146	0.3478 ± 0.0139	ULLD	ULLD	ULLD	5.2016 ± 0.0539
otis-II.5	0.0 ± 0.0	2.04 ± 0.3643	2.2828 ± 0.1206	1.4273 ± 0.0555	16.6443 ± 0.1007	5.7269 ± 0.0623	1.6301 ± 0.0382	63.3176 ± 0.1668	0.304 ± 0.0238	ULLD	0.1451 ± 0.0403	ULLD	5.6468 ± 0.0822
otis-II.6	0.0 ± 0.0	2.8234 ± 0.3371	10.4787 ± 0.1799	1.0256 ± 0.0527	8.3285 ± 0.0669	4.1976 ± 0.0478	3.6124 ± 0.0449	58.093 ± 0.1347	0.8213 ± 0.0204	ULLD	0.1557 ± 0.0322	0.1108 ± 0.0272	9.8054 ± 0.089
otis-II.7	0.0 ± 0.0	1.1856 ± 0.2249	3.5738 ± 0.0914	0.6603 ± 0.0322	21.9241 ± 0.0793	2.9471 ± 0.0338	1.1512 ± 0.0245	63.8889 ± 0.1153	0.2075 ± 0.0124	ULLD	ULLD	ULLD	3.8083 ± 0.0465
otis-III.1	0.0 ± 0.0	0.8766 ± 0.157	0.8765 ± 0.0474	0.4355 ± 0.0197	0.5575 ± 0.0121	1.21 ± 0.0142	ULLD	81.9518 ± 0.0931	11.5709 ± 0.0398	ULLD	ULLD	ULLD	2.1716 ± 0.0297

otis-III.2	0.0 ± 0.0	0.7861 ± 0.1699	0.9346 ± 0.0513	0.5035 ± 0.0218	0.5601 ± 0.0129	1.2462 ± 0.0151	ULLD	81.7436 ± 0.0979	11.5396 ± 0.042	ULLD	ULLD	ULLD	2.2215 ± 0.0318
otis-III.3	0.0 ± 0.0	1.1208 ± 0.1464	0.9329 ± 0.0457	0.489 ± 0.0196	0.5902 ± 0.0121	1.1963 ± 0.014	ULLD	82.1474 ± 0.0942	11.4708 ± 0.0401	ULLD	ULLD	ULLD	1.6628 ± 0.0264
otis-III.4	0.0 ± 0.0	1.1842 ± 0.1606	0.8739 ± 0.0481	0.5107 ± 0.021	0.5841 ± 0.0127	1.3706 ± 0.0154	ULLD	81.2011 ± 0.0971	11.7208 ± 0.0419	ULLD	ULLD	ULLD	2.1894 ± 0.0315
otis-III.5	0.0 ± 0.0	3.5205 ± 0.2006	9.5334 ± 0.1201	0.8418 ± 0.0272	1.2446 ± 0.0196	2.2377 ± 0.0228	2.41 ± 0.0235	72.7689 ± 0.109	0.539 ± 0.014	ULLD	0.0981 ± 0.02	0.1822 ± 0.0218	5.8993 ± 0.0541
otis-IV.1	0.0 ± 0.0	2.656 ± 0.2633	5.7127 ± 0.1137	0.9299 ± 0.0342	3.0382 ± 0.0429	0.0 ± 0.0233	1.503 ± 0.0194	78.1331 ± 0.1014	0.5024 ± 0.0221	ULLD	ULLD	0.1685 ± 0.0275	6.4983 ± 0.0865
otis-IV.2	9.913 ± 1.56	4.7873 ± 0.2264	8.7476 ± 0.1288	1.2563 ± 0.0322	2.2151 ± 0.0361	0.0 ± 0.0235	2.2636 ± 0.0232	63.5829 ± 0.0904	0.3922 ± 0.0185	ULLD	ULLD	0.1529 ± 0.0244	5.3562 ± 0.0723
otis-IV.3	0.0 ± 0.0	2.305 ± 0.298	4.375 ± 0.116	0.8197 ± 0.0375	1.8282 ± 0.0396	0.0 ± 0.0259	1.2773 ± 0.0202	83.3001 ± 0.1146	0.4108 ± 0.0244	ULLD	ULLD	ULLD	4.8671 ± 0.0841
otis-V.1	0.0 ± 0.0	0.6672 ± 0.1737	0.8866 ± 0.0544	0.636 ± 0.0268	10.9128 ± 0.0973	5.7472 ± 0.0444	ULLD	1.5314 ± 0.0157	3.2566 ± 0.0313	0.8415 ± 0.1284	11.1284 ± 0.114	ULLD	29.4212 ± 0.1362
otis-V.2	0.0 ± 0.0	0.6743 ± 0.1534	1.2605 ± 0.0511	1.1025 ± 0.0245	0.4989 ± 0.017	3.8487 ± 0.0214	ULLD	16.1946 ± 0.0272	2.2836 ± 0.0105	ULLD	3.6689 ± 0.039	0.4489 ± 0.0305	65.4413 ± 0.1313
anoeta	4.648 ± 0.7814	2.9065 ± 0.1495	4.2788 ± 0.0728	0.7772 ± 0.021	1.4438 ± 0.0176	1.5671 ± 0.0165	ULLD	81.2918 ± 0.1007	0.283 ± 0.0106	ULLD	0.0688 ± 0.0163	0.0416 ± 0.0126	2.3261 ± 0.0312
anoeta2	0.0 ± 0.0	2.4055 ± 0.1605	3.2999 ± 0.0682	0.7529 ± 0.0223	1.3428 ± 0.0174	1.4481 ± 0.0163	ULLD	87.9949 ± 0.1076	0.2435 ± 0.011	ULLD	0.0598 ± 0.0186	ULLD	2.1672 ± 0.032
anoeta3	0.0 ± 85.5969	1.978 ± 0.1922	4.0117 ± 0.0833	0.7219 ± 0.0262	1.5826 ± 0.0209	1.6823 ± 0.0194	0.8164 ± 0.0149	85.3071 ± 0.1136	0.3668 ± 0.0134	ULLD	0.0842 ± 0.0204	ULLD	3.2027 ± 0.0411
anoetahoe	0.0 ± 0.0	3.8531 ± 0.2006	10.5503 ± 0.1177	0.6515 ± 0.0252	0.5111 ± 0.0135	1.5102 ± 0.0181	3.9628 ± 0.0276	72.1582 ± 0.1008	0.4862 ± 0.0123	ULLD	0.071 ± 0.0178	0.0786 ± 0.0158	5.836 ± 0.0492
anoetahoe	0.0 ± 0.0	4.7065 ± 0.2057	14.3708 ± 0.1356	0.5927 ± 0.0262	0.5361 ± 0.0148	1.6912 ± 0.02	5.2998 ± 0.0326	64.4235 ± 0.096	0.7073 ± 0.0129	ULLD	0.0621 ± 0.0163	0.0977 ± 0.0163	7.1623 ± 0.0527
anoetahoe	0.0 ± 0.0	4.3802 ± 0.1938	10.7223 ± 0.1124	0.6028 ± 0.0231	0.5169 ± 0.0129	1.353 ± 0.0164	2.3462 ± 0.0205	72.9636 ± 0.0946	0.5878 ± 0.0119	ULLD	ULLD	0.1271 ± 0.0127	6.0906 ± 0.0473

Sample location	Inorganic compound (wt.%)												
	Co	Ni	Cu	Zn	Rb	Sr	Zr	Mo	Cd	Sn	Sb	Ba	Pb
otis-I.1	ULLD	ULLD	ULLD	0.0573 ± 0.003	0.0785 ±0.0022	0.6472 ±0.0043	0.0241 ±0.0025	ULLD	ULLD	ULLD	ULLD	0.128 ± 0.0316	ULLD
otis-I.1.humedo	ULLD	ULLD	0.0061 ± 0.002	0.0612 ±0.0028	0.0537 ±0.0018	0.6166 ±0.0039	0.0202 ±0.0022	ULLD	ULLD	ULLD	ULLD	0.1274 ±0.0279	ULLD
otis-I.2	ULLD	ULLD	0.0156 ±0.0027	0.1392 ±0.0041	0.0535 ±0.0019	0.7344 ±0.0046	0.0254 ±0.0027	ULLD	ULLD	ULLD	ULLD	0.1198 ±0.0309	ULLD
otis-I.3	ULLD	ULLD	ULLD	0.0717 ±0.0033	0.0523 ±0.0019	0.8079 ±0.0047	0.0278 ±0.0026	ULLD	ULLD	ULLD	ULLD	0.1013 ± 0.03	ULLD
otis-I.4	ULLD	ULLD	ULLD	0.1183 ±0.0039	0.052 ± 0.002	0.8177 ±0.0047	0.0247 ±0.0027	ULLD	ULLD	0.0291 ±0.0091	ULLD	0.1426 ±0.0321	ULLD
otis-I.5	ULLD	ULLD	ULLD	0.1101 ±0.0039	0.0627 ±0.0022	0.844 ± 0.005	0.0217 ±0.0028	0.0081 ±0.0022	ULLD	ULLD	ULLD	0.1614 ± 0.033	ULLD
otis-II.1	ULLD	ULLD	ULLD	0.0686 ±0.0054	0.0235 ±0.0034	0.2845 ±0.0051	0.0263 ±0.0043	0.0135 ±0.0044	ULLD	ULLD	0.0625 ±0.0201	ULLD	0.0456 ± 0.0071
otis-II.2	ULLD	ULLD	ULLD	0.0626 ±0.0042	0.0157 ±0.0026	0.2727 ±0.0041	0.0351 ±0.0035	0.0123 ±0.0034	0.0405 ±0.0114	0.0738 ±0.0145	0.0613 ±0.0158	0.1824 ±0.0509	ULLD
otis-II.3	ULLD	ULLD	ULLD	0.1003 ±0.0052	0.0353 ±0.0029	0.3116 ±0.0045	0.0441 ±0.0039	0.012 ± 0.0037	ULLD	ULLD	0.0677 ±0.0175	0.1794 ±0.0546	ULLD
otis-II.4	ULLD	ULLD	ULLD	0.076 ± 0.0043	0.0202 ±0.0024	0.1982 ±0.0035	0.0286 ± 0.003	ULLD	ULLD	ULLD	0.0478 ±0.0142	ULLD	ULLD
otis-II.5	ULLD	ULLD	ULLD	0.095 ± 0.0071	0.0233 ±0.0043	0.2946 ±0.0063	0.0394 ±0.0055	ULLD	ULLD	0.0762 ±0.0224	ULLD	0.2632 ±0.0763	0.0432 ± 0.0086
otis-II.6	ULLD	ULLD	ULLD	0.083 ± 0.0059	0.0368 ±0.0038	0.3616 ±0.0057	0.0659 ±0.0051	ULLD	ULLD	ULLD	ULLD	ULLD	ULLD
otis-II.7	ULLD	ULLD	ULLD	0.0733 ±0.0041	0.023 ± 0.0025	0.2957 ± 0.004	0.0342 ±0.0032	0.0136 ±0.0032	ULLD	0.0435 ±0.0139	ULLD	0.1699 ±0.0475	ULLD
otis-III.1	ULLD	ULLD	ULLD	0.0119 ± 0.0021	0.0068 ± 0.0017	0.29 ± 0.0032	0.0409 ± 0.0025	ULLD	ULLD	ULLD	ULLD	ULLD	ULLD
otis-III.2	0.0234 ±0.0065	ULLD	ULLD	0.0073 ±0.0024	ULLD	0.2731 ±0.0033	0.045 ± 0.0027	0.0086 ±0.0024	ULLD	ULLD	ULLD	0.1075 ± 0.034	ULLD

otis-III.3	ULLD	ULLD	ULLD	0.0089 ±0.0019	0.0051 ±0.0018	0.3016 ±0.0032	0.0447 ±0.0025	ULLD	ULLD	0.0296 ± 0.0094	ULLD	ULLD	ULLD
otis-III.4	0.0218 ±0.0067	0.0193 ±0.0035	ULLD	0.0148 ±0.0024	ULLD	0.2558 ±0.0032	0.0434 ±0.0027	0.01 ± 0.0024	ULLD	ULLD	ULLD	ULLD	ULLD
otis-III.5	ULLD	ULLD	ULLD	0.0169 ±0.0026	0.0231 ±0.0023	0.6318 ±0.0051	0.0406 ±0.0034	0.0121 ±0.0029	ULLD	ULLD	ULLD	ULLD	ULLD
otis-IV.1	ULLD	ULLD	0.0321 ± 0.006	0.0444 ±0.0055	ULLD	0.7468 ±0.0088	0.0347 ±0.0051	ULLD	ULLD	ULLD	ULLD	ULLD	ULLD
otis-IV.2	ULLD	ULLD	ULLD	0.0904 ±0.0059	0.0115 ±0.0036	1.1924 ±0.0096	0.0384 ±0.0042	ULLD	ULLD	ULLD	ULLD	ULLD	ULLD
otis-IV.3	ULLD	ULLD	0.0249 ±0.0071	0.0272 ±0.0063	ULLD	0.727 ± 0.0097	0.0377 ±0.0057	ULLD	ULLD	ULLD	ULLD	ULLD	ULLD
otis-V.1	0.2109 ±0.0232	ULLD	ULLD	0.0384 ±0.0078	0.0409 ± 0.005	0.0703 ±0.0055	0.112 ± 0.0069	0.0697 ±0.0072	ULLD	ULLD	ULLD	3.3755 ±0.3902	31.0532 ± 0.0887
otis-V.2	ULLD	ULLD	0.0916 ±0.0072	4.4565 ±0.0287	ULLD	ULLD	ULLD	ULLD	0.0299 ±0.0083	ULLD	ULLD	ULLD	ULLD
anoeta	ULLD	ULLD	ULLD	0.2605 ±0.0054	ULLD	0.1007 ±0.0022	0.0061 ±0.0019	ULLD	ULLD	ULLD	ULLD	ULLD	ULLD
anoeta2	ULLD	ULLD	ULLD	0.1026 ±0.0039	ULLD	0.1001 ±0.0024	ULLD	ULLD	ULLD	0.0494 ±0.0098	0.0333 ±0.0106	ULLD	ULLD
anoeta3	ULLD	ULLD	ULLD	0.0834 ± 0.004	ULLD	0.1127 ±0.0028	ULLD	0.0095 ±0.0025	ULLD	0.0405 ±0.0107	ULLD	ULLD	ULLD
anoetahoe	ULLD	ULLD	ULLD	0.1611 ±0.0048	0.026 ± 0.002	0.1291 ±0.0026	0.0148 ±0.0021	ULLD	ULLD	ULLD	ULLD	ULLD	ULLD
anoetahoe	ULLD	ULLD	ULLD	0.1836 ±0.0049	0.029 ± 0.002	0.1257 ±0.0025	0.0119 ±0.0022	ULLD	ULLD	ULLD	ULLD	ULLD	ULLD
anoetahoe	ULLD	ULLD	0.0068 ±0.0023	0.1596 ±0.0043	0.0164 ±0.0017	0.1133 ±0.0023	0.0137 ± 0.002	ULLD	ULLD	ULLD	ULLD	ULLD	ULLD

3.4.2. Number of samples and sample distribution

The sample pool for Task 2.3 strikes a balance between depth (laboratory samples with extensive characterisation) and breadth (in situ measurements providing extensive coverage of structures). As presented in Table 3, the laboratory dataset comprises of three powdered concrete samples and one asphalt sample, which were provided by MOYUA. These were processed under controlled laboratory conditions to serve as benchmark materials for reference analysis.

Table 3. Inorganic content of the received milled samples measured by portable and benchtop XRF.

Inorganic compounds (wt. %)	Sample name						
	Portable XRF			Benchtop XRF			
	Foso	Fresado	Columna	Foso	Fresado	Columna	Asphalt
Al	0.9713±0.0903	1.4217±0.1166	1.2038±0.1122	0.402	1.246	0.858	3.63
Si	1.3697±0.033	4.1946±0.0608	3.0945±0.0521	1.188	4.305	3.423	9.822
P	0.3959±0.012	0.5587±0.0172	0.4343±0.0156				
S	0.3777±0.007	0.7884±0.0117	1.8813±0.0162	0.133	0.352	1.299	5.812
Cl	0.689±0.0079	0.906 ± 0.0111	2.4705±0.0169	0.863	0.168	2.142	0.263
K	2.0541±0.0128	1.3321±0.0129	1.7589± 0.0149	2.259	1.443	2.042	0.925
Ca	54.8493±0.059	43.0682±0.0591	46.9203±0.0623	62.92	49.335	52.195	64.881
Ti	0.1752±0.0061	0.8625±0.0101	0.413±0.0082	0.183	0.897	0.43	0.664
V				0.01581	0.08689	0.02306	0.08464
Cr		0.0579± 0.0124	0.037±0.0116	0.00697	0.04402	0.01599	0.04865
Mn	0.1125±0.0083	0.1425± 0.0101	0.0827±0.0114	0.173	0.205	0.129	0.211
Fe	2.1032±0.0214	8.4363± 0.0457	5.0293±0.0358	2.46	9.786	5.698	13.285
Ni		0.0086± 0.0025		ULLD[a]	0.02244	ULLD[a]	0.04386
Cu		0.0094± 0.0022		ULLD[a]	0.02078	0.01543	0.02698
Zn	0.0332±0.0018	0.0358± 0.0023	0.089±0.0029	0.75	0.386	0.107	0.024
Ga				ULLD[a]	ULLD[a]	0.00359	
As				ULLD[a]	0.00391	0.01861	
Br				ULLD[a]	ULLD[a]	0.01379	
Rb	0.0206±0.0011	0.0098± 0.0014	0.0185±0.0014	0.03646	0.01734	0.02947	0.00631
Sr	0.7518±0.0034	0.1605± 0.0022	0.1725±0.0022	1.072	0.228	0.239	0.144
Y				0.00348	0.00625	0.00536	
Zr	0.0152±0.0017	0.028 ± 0.0019	0.0316±0.0019	0.02038	0.04596	0.02962	0.03021
Mo		0.0081± 0.0018	0.0056±0.0017				
Cd		0.0209±0.006					
Sn	0.0238±0.0053	0.0289± 0.0076		0.02374	0.0176	0.05127	0.03694
Ba	0.1096±0.0184	0.09±0.0259	0.1289±0.0237	148	ULLD	ULLD	
Pb		0.0081±0.0026		0.05127	0.01087	0.05127	

[a] ULLD: Under lower limit of detection

Funded by the European Union

Alongside these laboratory samples, the field campaign in April 2025 produced 29 p-XRF measurements across two demonstrators. Five different structural zones were targeted at the OTIS factory, including walls, columns, and beams. These elements were selected for their structural relevance and visible surface features, such as efflorescence, cracks and corrosion marks, which could potentially alter surface-sensitive XRF readings (see Figure 4). At Anoeta Stadium, the asphalt zone was selected as being representative of road and pavement materials within the transport infrastructure, a category that is highly relevant to the project's demonstrator objectives.

Figure 4. Salt efflorescence on Area II

Figure 5 visualises the measurement distribution and shows photographs of the measurement points and the conditions under which they were acquired. This documentation provides traceability and contextual information to help interpret variability in the dataset. Moreover, to address heterogeneity and evaluate reproducibility, triplicate measurements were performed at several points. Samples collected for laboratory analysis were subdivided into aliquots, enabling parallel testing with EDXRF, ICP-OES and XRD without the risk of cross-contamination.

Funded by
the European Union

Figure 5. From top left to bottom right. Area I: Spot measurements from right to left. Area II: Spot measurements from right to left (areas with salt efflorescence are visible all along the wall and corner). Area III: Spot measurements from right to left. Area IV: Spot measurements from right to left. Area V: Spot 1 yellow beam and spot 2 green beam. Area VI: Anoeta asphalt measurement area.

3.4.3. Quality assurance and control measures

The reliability of the dataset was underpinned by strict QA/QC procedures. Calibration of both the EDXRF and p-XRF was carried out using the SOILS-LE calibration program, which applies the FPs method to correct for matrix effects. To verify accuracy and monitor drift, CRMs were employed. These were pressed into 32 mm pellets and analysed systematically at the start and end of each measurement sequence, providing clear benchmarks for evaluating instrument stability.

Reproducibility was ensured by performing triplicate measurements on each laboratory sample and calculating relative standard deviations (Table 3). These results confirmed that the analytical precision of the EDXRF was within acceptable limits for construction materials. The portable system was likewise tested for stability by repeating spot measurements in the field.

To address the inherent matrix effects of concrete and asphalt, such as spectral overlaps, absorption and enhancement phenomena, ICP-OES was included as a bulk reference technique. Microwave digestion using the ETHOS EASY system ensured the complete dissolution of the silicate and carbonate phases, and the ICP-OES provided highly sensitive and accurate quantification of both the major and trace elements. In parallel, XRD was used to identify crystalline phases (Figure 6), which were crucial for interpreting discrepancies between the surface-sensitive XRF and the bulk-sensitive ICP-OES techniques. For instance,

Funded by
the European Union

the presence of portlandite or calcite, as identified by XRD, directly explained variations in the Ca/Si ratio reported by XRF.

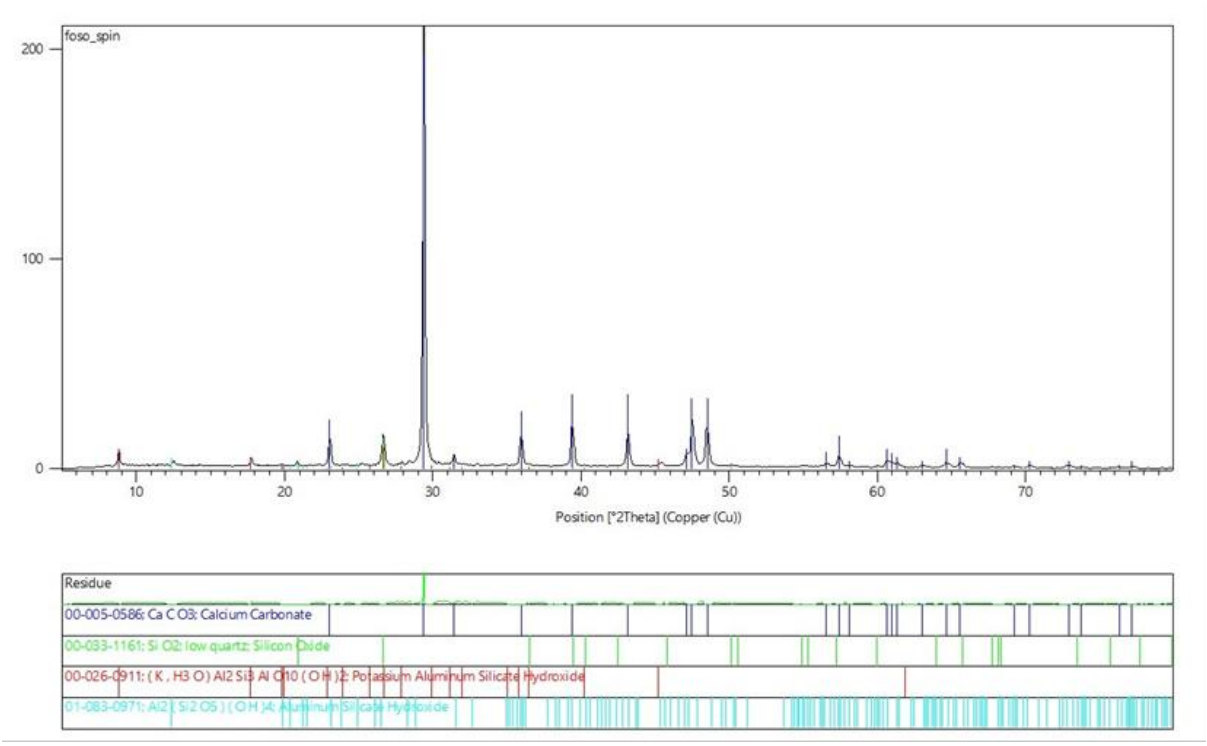

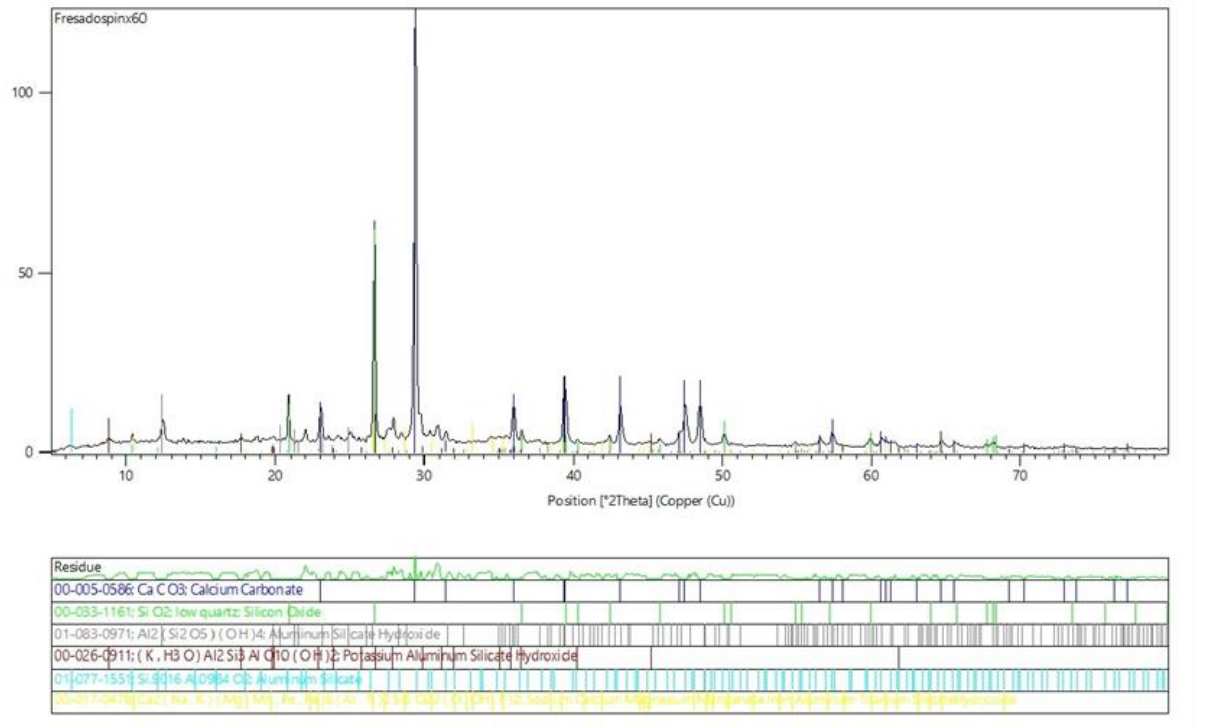

Funded by
the European Union

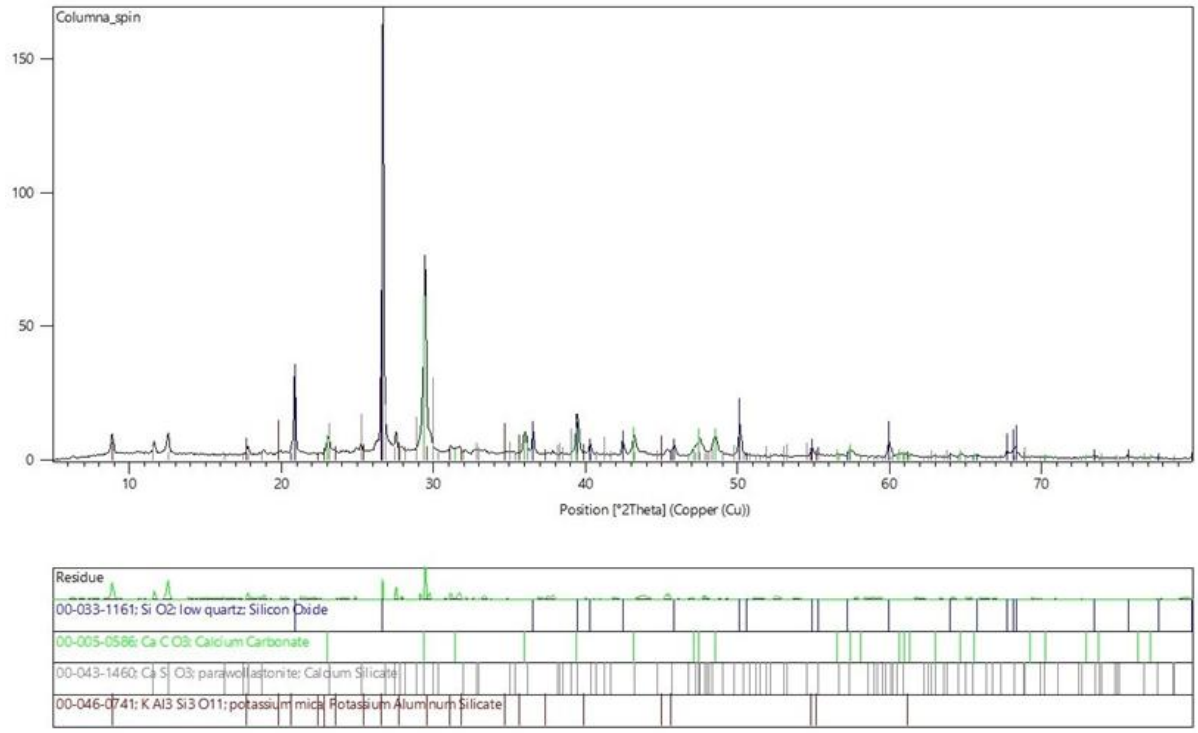

Figure 6. XRD diffractograms of concrete samples obtained from Foso, Fresado and Columna

3.4.4. Procedure for data acquisition

The acquisition procedure followed a harmonised, multi-step workflow. In the field, p-XRF was used to acquire elemental profiles at systematically defined points. Each location was documented with photographs (Figure 5), while metadata such as acquisition time, instrument ID, operator and environmental conditions were logged in a standardised format. Where possible, surfaces were cleaned to remove dust and loose coatings, and care was taken to avoid measuring cracks or irregular areas that could distort the results.

Representative bulk fragments of materials (100–200 g) were collected from the same areas that were surveyed by p-XRF. These were then dried, ground and sieved in the laboratory to obtain a homogeneous powder. Subsamples were then pressed into pellets for EDXRF analysis. Thereby ensuring reproducibility and comparability across instruments.

In parallel with XRF analysis, subsamples were prepared for ICP-OES. Complete digestion was achieved using the ETHOS EASY microwave system under high-pressure closed vessel conditions to guarantee that the silicate and carbonate phases were fully dissolved. The digested solutions were analysed using the CP-OES, which provided accurate concentrations of both major and trace elements at the bulk level. Additionally, powdered subsamples were analysed by XRD to determine the crystalline phases present using diffraction pattern matching against the ICDD database (Figure 6).

3.4.5. Development and Validation of ML Regression Models

The final stage of Task 2.3 involved developing machine learning (ML) regression models for material identification. The aim was to create predictive frameworks that could convert rapid, surface-sensitive XRF measurements into accurate elemental compositions at a bulk level, as validated against ICP-OES reference data. This approach overcomes the limitations of XRF, such as shallow penetration depth, matrix effects and the difficulty of quantifying light elements, by training models to learn non-linear corrections directly from paired datasets.

The dataset collected in this work was comprehensive. It drew on the harmonized mineral composition database, which contains elemental ranges for cement binders, aggregates of

Funded by
the European Union

different lithologies, and heavy metals found in cement and asphalt. Values for the major elements (Ca, Si, Al, Fe and Mg) were extracted from both cement and aggregate records, while values for the hazardous elements (Pb, Cr, Ni, Zn and Cu) were integrated through the dedicated heavy metals sheet. Consistent application of conversion factors from oxides to elemental values was used to standardise the dataset, and oxygen content was calculated by closure to achieve 100% mass balance. These curated datasets were then linked with ICP-OES measurements of digested samples, providing the necessary ground for future regression learning.

The patterns inherent in the dataset become apparent when visualising the major binders. Figure 7 shows the relationship between calcium and silicon content in cement, emphasising the compositional variations that distinguish different cement chemistries. The Ca–Si relationship was a central feature leveraged by the regression models as it correlates strongly with mechanical and durability properties. These chemical trends provided a basis for the algorithms to capture.

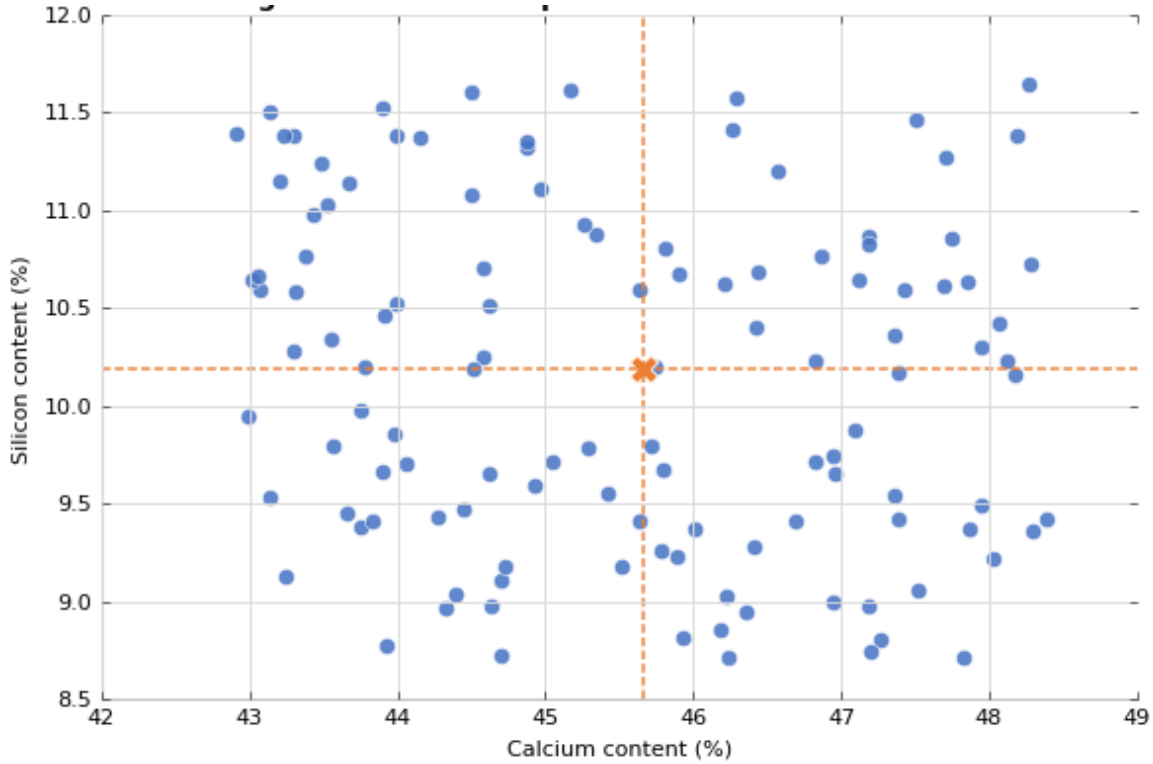

Figure 7. Relationship between calcium and silicon contents in cement, showing compositional trends used in modelling where the average is represented by an orange cross means and the used data is represented in a blue colour.

Concurrently, a rigorous analysis of hazardous elements was conducted to ensure that the models possessed not only the capacity to classify materials but also the capability to detect regulatory thresholds for contaminants. As it is shown in Figure 8, the mean concentrations of heavy metals in cement are expressed as percentages. The findings indicate that, while lead and chromium are generally present at low levels, there are instances where they can exceed critical thresholds. The integration of these elements into the regression models enabled the system to identify potentially hazardous materials, thereby supporting compliance with the requirements of the EU Waste Framework Directive. The ML models that were tested included linear regression and partial least squares regression (PLSR) as baselines, random forest regression (RFR) as a robust ensemble method, support vector regression (SVR) to capture high-dimensional non-linearities, and artificial neural networks (ANNs) that were optimized for element prediction across complex matrices. The dataset was segmented into a training

Funded by
the European Union

subset (70%) and a validation subset (30%), with five-fold cross-validation employed to evaluate the generalisation capability. Hyperparameters were tuned through grid search optimization, with the number of estimators, kernel type, and learning rate adjusted for each method.

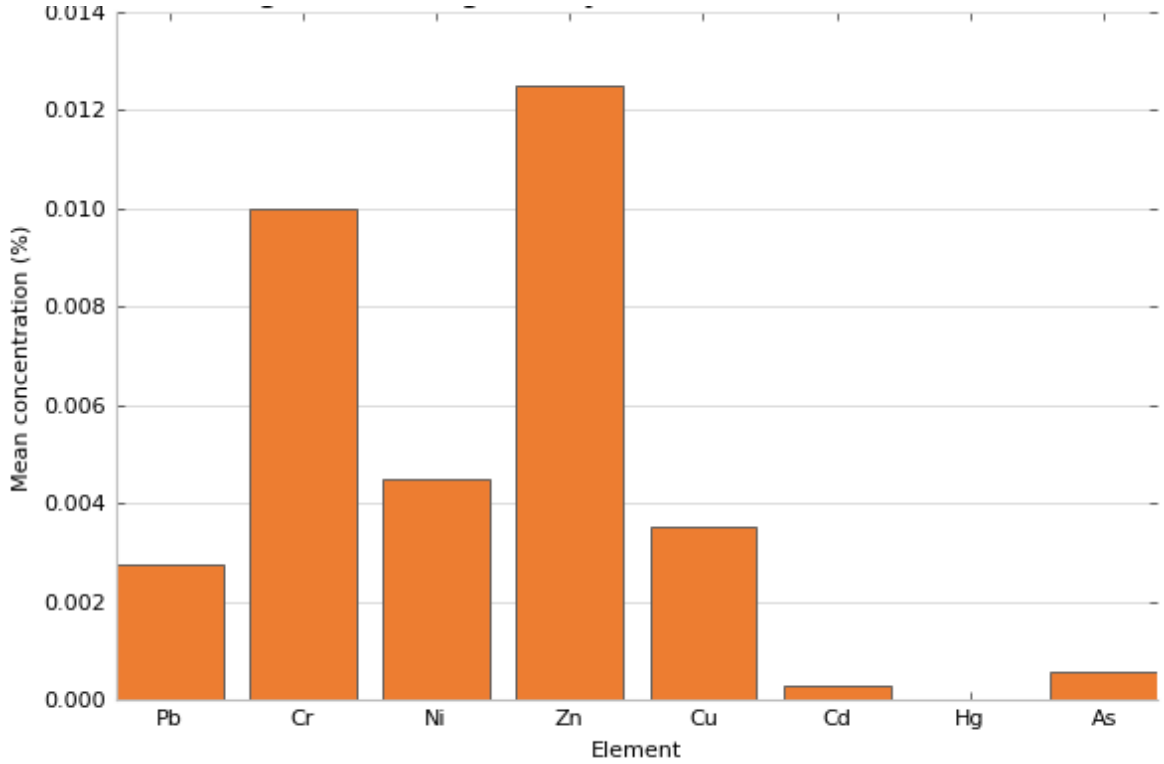

Figure 8. Average heavy metal concentrations (Pb, Cr, Ni, Zn, Cu, Cd, Hg and As) in cement, highlighting regulatory-relevant elements.

The comparative performance of these models is summarised in Figure 9, which shows the coefficient of determination (R^2) values obtained during validation. Linear models demonstrated an inability to adequately capture the complexity of the data, with R^2 values falling below 0.80. In contrast, RFR attained $R^2 > 0.92$ for major oxides, while ANNs achieved R^2 values exceeding 0.90 for trace heavy metals such as Pb and Zn. Furthermore, the SVR model demonstrated notable efficacy, particularly in the analysis of chromium and nickel, where kernel-based methods exhibited superiority in capturing non-linear relationships.

The findings indicate that linear approaches are inadequate for construction material datasets, while ensemble and neural network methods ensure highly reliable predictions. For instance, RFR successfully predicted Ca, Si, and Al concentrations in cement with relative errors of less than 3% compared to ICP-OES references. In contrast, ANNs demonstrated optimal accuracy for hazardous trace elements, where non-linear effects prevail.

Subsequently, the validated models were applied to classification tasks. Utilising the same integrated dataset, the framework distinguished between concrete, asphalt, and masonry fractions with 96% overall accuracy. This classification capacity is of particular value in demolition and renovation projects, where mixed materials must be rapidly sorted. Furthermore, the models demonstrated a high degree of reliability in identifying hazardous samples, such as cement with Pb >0.01% or Cr >0.02%, thus facilitating on-site risk management.

Funded by
the European Union

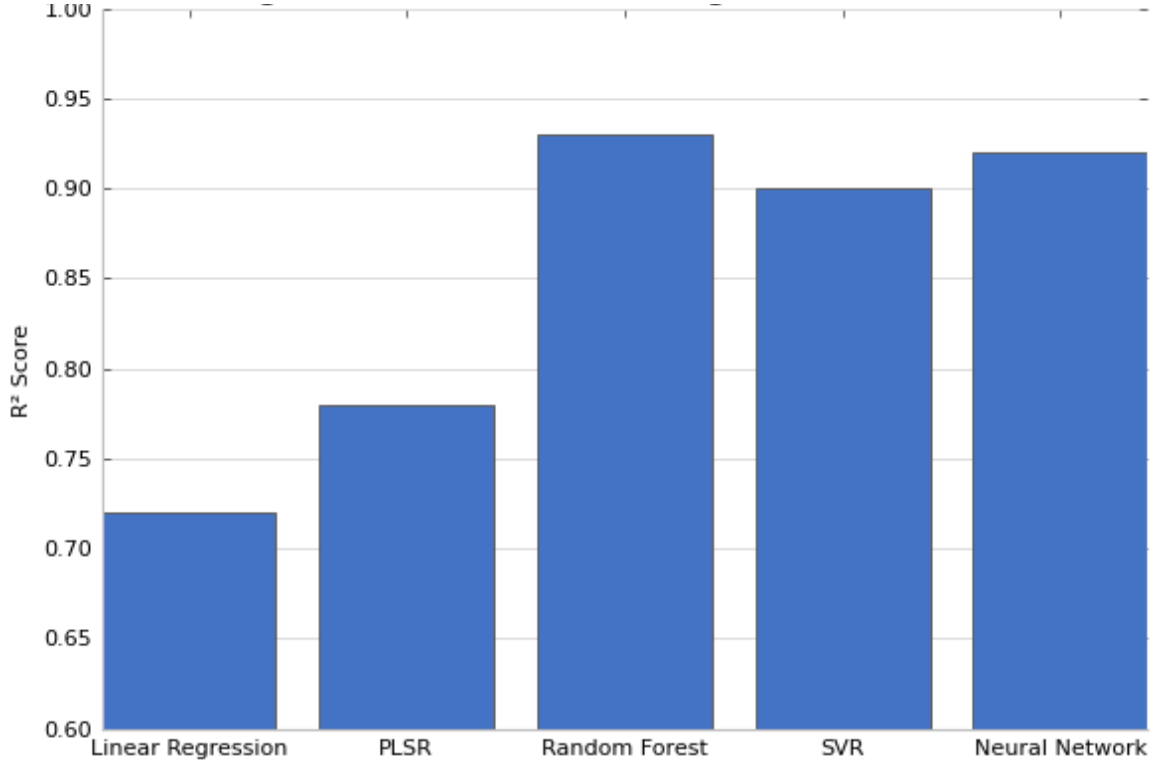

Figure 9. Performance benchmark of ML regression models (Linear, PLSR, Random Forest, SVR, Neural Network), showing Random Forest and Neural Networks as top performers ($R^2 > 0.90$).

The development of these models also yielded several significant insights. Firstly, it was determined that dataset diversity was of critical importance. The incorporation of both raw aggregates and finished materials (i.e., cement, asphalt) resulted in the models demonstrating superior capacity for generalisation across material classes. Secondly, non-linear algorithms such as ANNs and SVR demonstrated particular strengths in the prediction of trace contaminants, while ensemble approaches, including random forest, exhibited superior performance in the prediction of major oxides. Thirdly, the quantification of uncertainty emerged as a necessary complement. By aggregating predictions across multiple models, confidence intervals could be attached to predictions, thus helping operators to distinguish between results with high confidence and those that with low confidence. Finally, incorporating mineralogical descriptors from XRD into the feature set is expected to further improve accuracy, particularly for concrete, where crystalline phases significantly influence XRF signals.

The final framework has now been prepared for operational deployment in WP10 demonstrators in San Sebastián, in collaboration with MOYUA. In practice, portable XRF measurements collected at sites such as the Anoeta Station or the Jolastokieta industrial factory will be fed directly into the trained ML models, producing real-time estimates of bulk composition and hazard flags. This integration serves to close the methodological loop established in Task 2.3, thereby ensuring a seamless progression from systematic sampling and laboratory validation to the creation of an AI-driven decision-support tool.

Funded by
the European Union

3.5. Human resources assignment and roles

Table 4. Human resources

	Affiliation	Role	Contact info (mail)
Pablo José Arauzo Gimeno	OLAR	Supervision and performance of ICP analysis	Pj.arauzo@olar-solutions.com
Maciej Pawel Olszewski	OLAR	Performance of the XRF analysis	m.olszewski@olar-solutions.com
Jon Zubizarreta	MOYUA	Support related to the built environment and objectives of case study in Spain.	jon.zubizarreta@etra.eus

3.6. Scheduling

T2.3.1 Design basis of methodology and calibration analysis (M3 to M7)

T2.3.2 Collection and pre-treatment of the samples from the Spanish Pilot Site (M7 to M8)

T2.3.3 Performance of the analysis in laboratory prior pilot site (M8 to M11)

T2.3.4 Data Collection in San Sebastian with portable XRF (M11)

T2.3.5 Perform of ICP-OES and verification (M11 to M14)

T2.3.6 Development of ML regression models for material identification (M11 to M14)

T2.3.7 Report writing and review (M14 to M17)

	2024					2025									
	Aug	Sep	Oct	Nov	Dec	Jan	Feb	Mar	Apr	May	Jun	Jul	Aug	Sep	Oct
	M3	M4	M5	M6	M7	M8	M9	M10	M11	M12	M13	M14	M15	M16	M17
T2.3.1															
T2.3.2															
T2.3.3															
T2.3.4															
T2.3.5															
T2.3.6															
T2.3.7															

Funded by the European Union

3.7. Critical tasks and milestones

3.7.1. Critical Tasks

Critical Task 2	Probability	Impact
Different testing materials are not available for verification due to logistics	Med	Med
Contingency		
Investigated materials will be decided before testing and distributed to all participants in due time.		

The materials were identified in advance by the company with the pilot site (i.e., MOYUA). The details of the locations where the analyses were performed are also similar with other tasks inside of the WA2. Data collection in the pilot site was smooth.

Critical Task 3	Probability	Impact
The contamination of the samples for analysis might affect to the accuracy and reliability of the data	Low	High
Contingency		
Implementation of tailored protocol for the sample handling, preparation, and analysis. Regular cleaning and maintenance of the XRF equipment.		

The initial samples analysed in the laboratory XRF were pre-treated to ensure the removal of the humidity that might affect the measurements. Moreover, in the pilot site, the locations of the measurements were brushed prior to the analysis to ensure that the dust or other non-desired pollutants (i.e., salt crystals) will not affect the measurement.

Critical Task 4	Probability	Impact
The processing of huge amounts of raw data (e.g., AHS, XRF) can lead to incorrect conclusions	Low	High
Contingency		
Develop and implement an automated data pre-processing by skilled data scientists with experience in handling large datasets.		

Although, a lot of samples were analysed in the Task 2.3, there was a screening of the most suitable ones for the data basis that will be used in the Task 3.3 for the development of the material prediction model. Moreover, the ICP-OES technique was used to verify the obtained results with p-XRF.

Critical Task 5	Probability	Impact
Technical limitations or malfunctions in the equipment (i.e., AHS, XRF) could lead to incomplete or erroneous data collection	Low	High

Funded by
the European Union

Contingency
Regularly maintenance and calibration of the equipment to ensure optimal performance and accuracy. Additionally, a backup of the equipment available in case of any technical failure.

The laboratory XRF and ICP has continuous calibrations to ensure the correct analysis of the sample. Whilst the p-XRF has also continuous calibrations as can be seen in the Appendix Figure A2.

3.7.2. Milestones

- AI models for material detection in the field (M17)

Verification form: Algorithms and laboratory results (D2.1 to 2.6) completed.

D2.3 (together with the other WP2 deliverables) ensures that there is sufficient data on which to train and test the WP3 AI algorithms. Thus, the complementation with open datasets ensures the smooth operation of WP3 and of the project.

3.8. Hardware

The execution of Task 2.3 required deployment of a suite of advanced analytical instruments, covering field-based screening and laboratory reference techniques. The hardware was selected to complement surface-sensitive and bulk-sensitive methods, enabling robust ML models to be developed for material identification.

For field acquisition, the project used the Oxford Instruments X-MET 7500 p-XRF. This handheld device is equipped with a rhodium (Rh) anode X-ray tube, a high-resolution SDD and an automatic five-position filter changer. It provides a wide elemental detection range (Mg to U) with acquisition times as short as 60 seconds per spot. Its robust design, integrated GPS and long-life battery made it ideal for rapid, non-destructive measurements at the San Sebastián pilot sites (Anoeta Station and the OTIS factory).

For laboratory-based XRF validation, a Malvern Panalytical Epsilon 1 EDXRF was used. This instrument features a Rh X-ray tube and a high-resolution SDD and employs the SOILS-LE calibration programme based on FPs. It was configured to analyse pressed pellets of construction materials (32 mm in diameter) to ensure reproducibility and comparability with the p-XRF data. The Epsilon 1 provided high-precision elemental profiles that served as the benchmark dataset for validating p-XRF performance.

To obtain bulk reference compositions, the project used an iCAP 7200 ICP-OES Duo spectrometer (manufactured by Thermo Fisher Scientific) coupled with a Milestone ETHOS EASY microwave digestion system. The ICP-OES offers dual axial and radial plasma viewing across a spectral range of 166–847 nm, with detection limits down to µg/L levels. It was used to quantify major and trace elements in fully digested concrete and asphalt samples, thereby providing the ground-truth data necessary to train the regression models. The ETHOS EASY digestion system ensured complete matrix dissolution by operating under controlled high-pressure and high-temperature conditions, with real-time monitoring of temperature and pressure inside closed vessels.

Phase identification was performed using a Bruker D2 Phaser 2nd Generation powder XRD. This benchtop diffractometer is equipped with a Cu Kα radiation source (λ = 1.5406 Å) and a LYNXEYE-2 position-sensitive detector. The instrument covered a 2θ range of 5° to 90°, and phase matching was conducted against the ICDD database. This enabled crystalline phases to be identified (e.g., portlandite, calcite, quartz and feldspars) in concrete and asphalt powders, providing a mineralogical context for the elemental analyses.

Together, these instruments formed a multi-tiered analytical platform: the portable XRF ensured rapid in situ screening, the laboratory XRF provided stable, high-quality reference

Funded by
the European Union

spectra, the ICP-OES delivered accurate elemental concentrations at the bulk level, the microwave digestion system guaranteed complete sample preparation and the XRD supplied mineralogical context. This integrated hardware configuration was essential for acquiring the datasets that underpinned the ML regression modelling, ensuring both accuracy and traceability.

3.9. Software

A combination of instrument-specific software for data acquisition and pre-processing, and scientific computing environments for advanced data analysis and ML model development supported the analytical and computational work carried out in Task 2.3.

For the XRF data acquisition and pre-processing, dedicated manufacturer software was used to operate both portable and laboratory instruments. The p-XRF (Figure 10) was controlled using X-MET Smart Data Transfer software, enabling real-time acquisition and metadata logging (including GPS coordinates), as well as the secure export of field measurements in CSV and PDF formats. The Malvern Panalytical Epsilon 1 EDXRF analyser was operated using the Omnian and SuperQ software suites, which include the SOILS-LE FPs calibration module. This ensured that spectral deconvolution, background subtraction and matrix corrections were performed consistently and in a traceable manner.

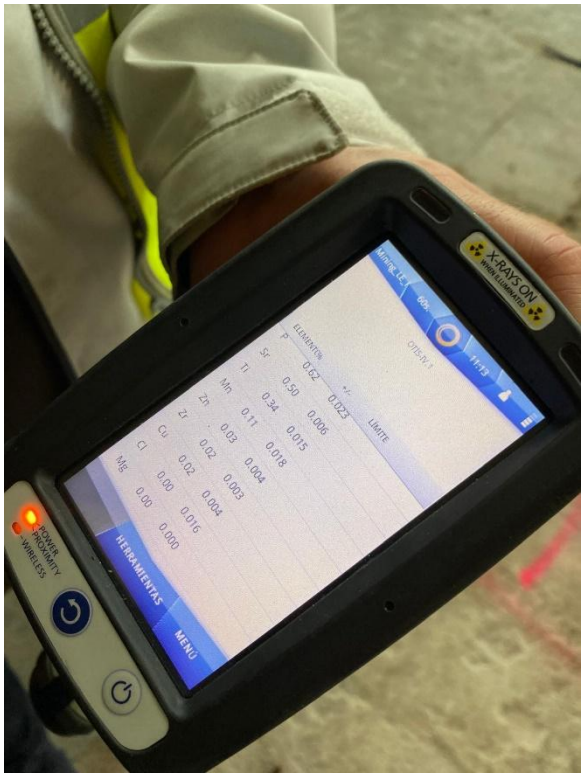

Figure 10. Software of data acquisition p-XRF

The Thermo Fisher iCAP 7200 Duo ICP-OES instrument was operated using the Qtegra Intelligent Scientific Data Solution (ISDS) software platform. This software enabled multi-element calibration using National Institute of Standards and Technology (NIST)-traceable standards, real-time plasma stability monitoring, and automated drift correction. The software was integrated with the Milestone ETHOS EASY digestion system. The system's EasyCONTROL software provided closed-vessel digestion programme design and real-time feedback on the temperature and pressure inside each vessel, thereby guaranteeing reproducibility.

Funded by
the European Union

For XRD phase identification, the Bruker D2 Phaser system was run using DIFFRAC.SUITE EVA software. This platform enabled automated phase identification by matching experimental diffraction patterns with entries in the ICDD database. The software's semi-quantitative Rietveld refinement tools were employed to analyse complex mixtures present in concrete powders and asphalt samples.

Beyond instrumental software, the development of ML regression models for material identification was carried out using open-source Python-based data science environments. The main tools included:

- Python 3.10 with Jupyter Notebook as the computational environment for reproducible workflows.
- NumPy and pandas for numerical computing and dataset pre-processing.
- scikit-learn for regression modelling (Linear Regression, PLSR, Random Forest, SVR), hyperparameter tuning, and cross-validation.
- TensorFlow/Keras for developing and training shallow ANNs, optimized for predicting both major oxide concentrations and trace heavy metal contents.
- Matplotlib and Seaborn for visualization, including scatterplots of compositional trends, bar charts of heavy metal contents, and performance benchmarking of regression models.

This computational environment ensured that raw XRF and ICP-OES data could be transformed into machine-readable formats, pre-processed for outlier detection and normalization, and finally used to train, validate, and benchmark ML models.

4. Challenges and limitations

4.1. Technical constraints of the technology

Although XRF and ICP-OES are well-established and complementary techniques, there are inherent technical constraints when using them in the context of CDW management.

XRF is fundamentally surface-sensitive, with penetration depths of only a few micrometres for heavy elements and up to 1–2 mm for light elements in low-density matrices. This limits its capacity to detect subsurface heterogeneity, especially in materials like concrete, where coatings, carbonation layers or corrosion residues may obscure the overall composition. Additionally, XRF does not provide molecular or crystallographic information, meaning polymorphs or mineral phases cannot be distinguished without additional XRD analysis. Spectral overlaps (e.g., between the Pb Lα and As Kα lines) further complicate the quantification of trace elements, particularly in heterogeneous or multi-element samples.

While ICP-OES is highly accurate, it requires destructive sample preparation via acid digestion. For silicate-rich concretes and carbonate-based mortars, achieving full dissolution can be time-consuming and requires careful optimisation of the protocol to avoid incomplete digestion or volatilisation losses. Using strong acids under high pressure also introduces safety and regulatory challenges.

Although XRD is powerful for phase identification, it has a limited detection threshold for minor phases (2–3 wt.%) and cannot easily quantify amorphous components such as hydrated cement gels. This restricts its ability to fully characterise disordered materials.

Therefore, while the technological platform is robust, the inherent limitations of each instrument must be addressed through methodological design and data integration.

4.2. Technical constraints of the proposed methodology

In addition to the limitations of the instruments used, the methodology developed in Task 2.3 was also subject to constraints that shaped the scope of the results.

Funded by
the European Union

While the sampling strategy was systematic, it was necessarily limited by access conditions at the pilot sites. For instance, safety and accessibility issues in the underground tunnel at Anoeta Station limited the number of measurement points and the ability to sample deeper structural layers. Similarly, while the OTIS factory offered large exposed concrete surfaces, many areas showed efflorescence or corrosion, which biased surface-sensitive XRF readings. Although triplicate measurements were used to mitigate this issue, residual variability remains.

The size of the dataset is another limitation. While the mineral composition database provided a broad reference range for cement, aggregates and heavy metals, the number of samples analyzed in the laboratory (approximately four for cement and asphalt in this phase) was relatively small. This restricts the statistical robustness of model training, particularly for trace elements where variability is high. To improve generalizability, it will be necessary to expand the dataset with additional samples across different construction typologies.

Integrating XRF with ICP-OES and XRD also presents challenges. Surface–bulk correlations are not always linear, and ML regression models must learn corrections influenced by both elemental composition and mineralogical context. Although RFR and ANN models achieved high predictive accuracy ($R^2 > 0.90$ for major oxides), their performance depends on the data and may deteriorate when applied to material types that are underrepresented in the training dataset.

Finally, the computational workflow itself has limitations. Although Python-based libraries such as scikit-learn and TensorFlow offer powerful modelling capabilities, training neural networks on relatively small datasets risks overfitting. In addition, quantifying uncertainty remains challenging; while ensemble averaging can mitigate some variability, it does not fully capture confidence in predictions.

Funded by
the European Union

5. Conclusion

Deliverable D2.3 has demonstrated the feasibility and effectiveness of integrating p-XRF, laboratory XRF, ICP-OES and XRD within a harmonised methodological framework for characterising construction and demolition materials. By combining fast, non-destructive field screening with accurate laboratory analyses of bulk samples, the project has generated a robust dataset that can be used to develop advanced ML models.

The results confirm that ML regression approaches, particularly RFR and ANNs, can successfully translate surface-sensitive XRF data into bulk compositional predictions with high accuracy ($R^2 > 0.90$). Furthermore, the models achieved 96% classification accuracy in distinguishing between concrete, asphalt and masonry while reliably identifying hazardous materials according to EU regulatory thresholds. These achievements validate the core objective of Task 2.3: enabling real-time, AI-assisted material identification at demolition and renovation sites.

However, the deliverable also identifies several challenges and limitations of the approach. These include the surface sensitivity of XRF, the complexity of matrix digestion for ICP-OES, the limited detection of amorphous phases by XRD and the relatively small size of the current training dataset. Addressing these issues will be essential for scaling up and generalising the methodology beyond the initial demonstrators.

Overall, the work reported here provides a solid technical foundation for the next phases of the project. The methodological framework, validated datasets and trained ML models are now ready to be deployed in WP10 demonstrators, where their applicability will be tested in real-world renovation and recycling scenarios. By doing so, D2.3 will contribute directly to the project's overarching aim of creating intelligent, circular and sustainable solutions for construction material management.

Funded by
the European Union

BIBLIOGRAPHY

Brouwer, P. N. (2010): Axios Max: Theory of XRF - Getting Acquainted with the principles. Available online at https://www.chem.purdue.edu/xray/docs/Theory%20of%20XRF.pdf, checked on 24-Sep-25.

Marjanovic, Ljiljana; McCrindle, Robert I.; Botha, Barend M.; Hermanus Potgieter, J. (2000): Analysis of cement by inductively coupled plasma optical emission spectrometry using slurry nebulization. In Journal of Analytical Atomic Spectrometry 15 (8), pp. 983–985. DOI: 10.1039/B003892J.

Mijatović, Nevenka; Terzić, Anja; Pezo, Lato; Miličić, Ljiljana; Živojinović, Dragana (2019): Validation of energy-dispersive X-ray fluorescence procedure for determination of major and trace elements present in the cement based composites. In Spectrochimica Acta Part B: Atomic Spectroscopy 162, p. 105729. DOI: 10.1016/j.sab.2019.105729.

Thermo Fisher Scientific (2025): iCAP PRO Series ICP-OES Typical Detection Limits. Available online at https://documents.thermofisher.com/TFS-Assets/CMD/Technical-Notes/tn-73452-icp-oes-icap-pro-detection-limits-tn73352-en.pdf, checked on 24-Sep-25.

U.S. Environmental Protection Agency (2007): Method 6200: Field portable X-ray fluorescence spectrometry for the determination of elemental concentrations in soil and sediment (SW-846 Physical/Chemical Methods). Available online at https://www.epa.gov/sites/default/files/2015-12/documents/6200.pdf, checked on 24-Sep-25.

U.S. Environmental Protection Agency. (2023): Field X-ray fluorescence (XRF) measurement: Operating procedure, LSASDPROC-107-R6 (EPA Region 4, Laboratory Services & Applied Science Division). Available online at https://www.epa.gov/sites/default/files/2016-01/documents/field_xrf_measurement107_af.r3.pdf, checked on 24-Sep-25.

U.S. Environmental Protection Agency. (2024): Field X-ray fluorescence measurement: SESD Field X-ray fluorescence measurement: SESD Operating Procedure 107-R4. Available online at https://19january2021snapshot.epa.gov/sites/static/files/2016-01/documents/field_xrf_measurement107_af.r3.pdf, checked on 24-Sep-25.

Zhen L. (2024): Using the Portable XRF to Identify/Verify Field Material Properties. Available online at https://ltrc.lsu.edu/pdf/2024/FR_691.pdf, checked on 24-Sep-25.

Funded by
the European Union

SUM4Re

Creating materials banks
from digital urban mining

APPENDICES

Funded by the European Union. Views and opinions expressed are however those of the author(s) only and do not necessarily reflect those of the European Union. Neither the European Union nor the granting authority can be held responsible for them.

Funded by
the European Union

LIST OF APPENDICES

LIST OF FIGURES IN THE APPENDICES

APPENDIX A Supplementary information of XRF

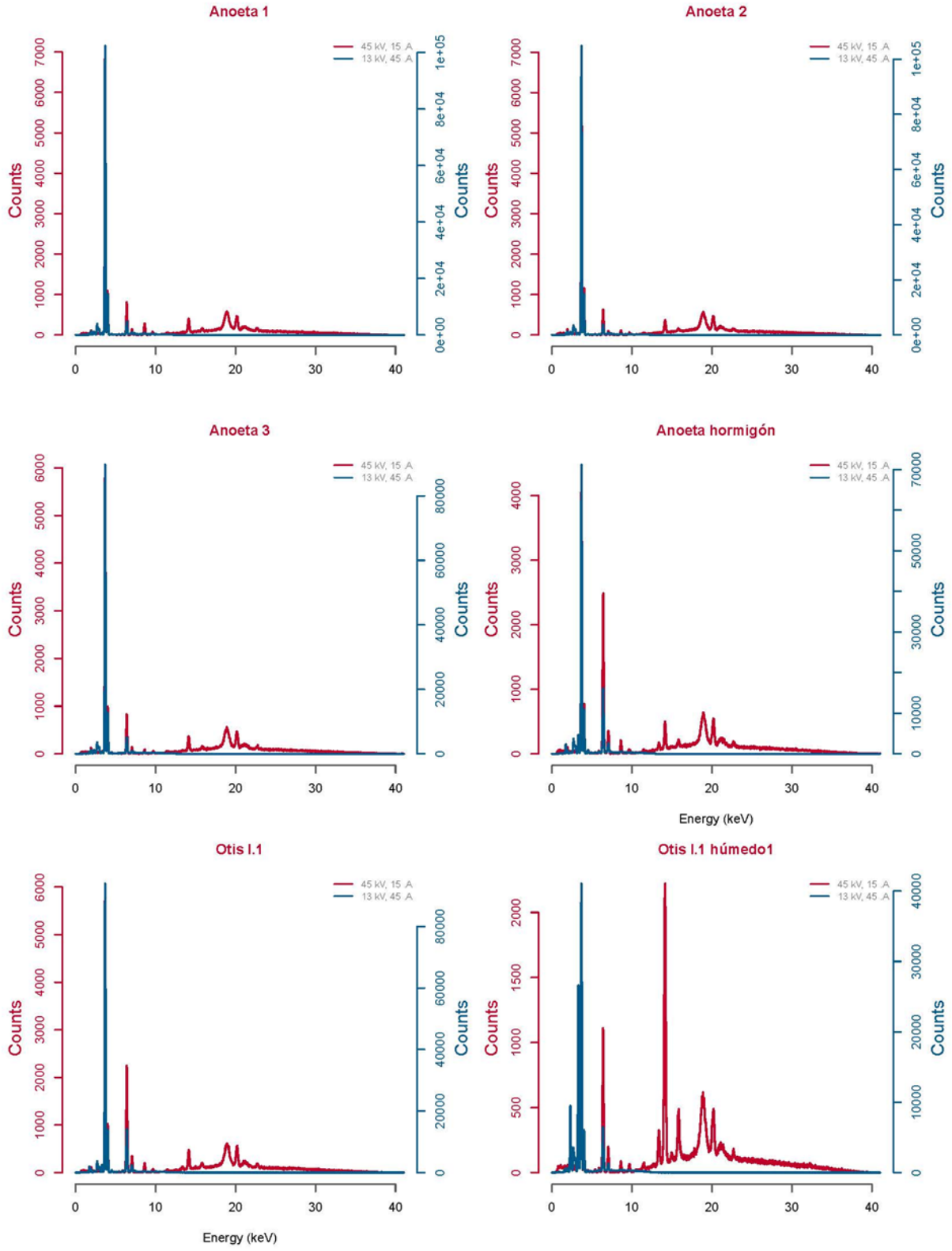

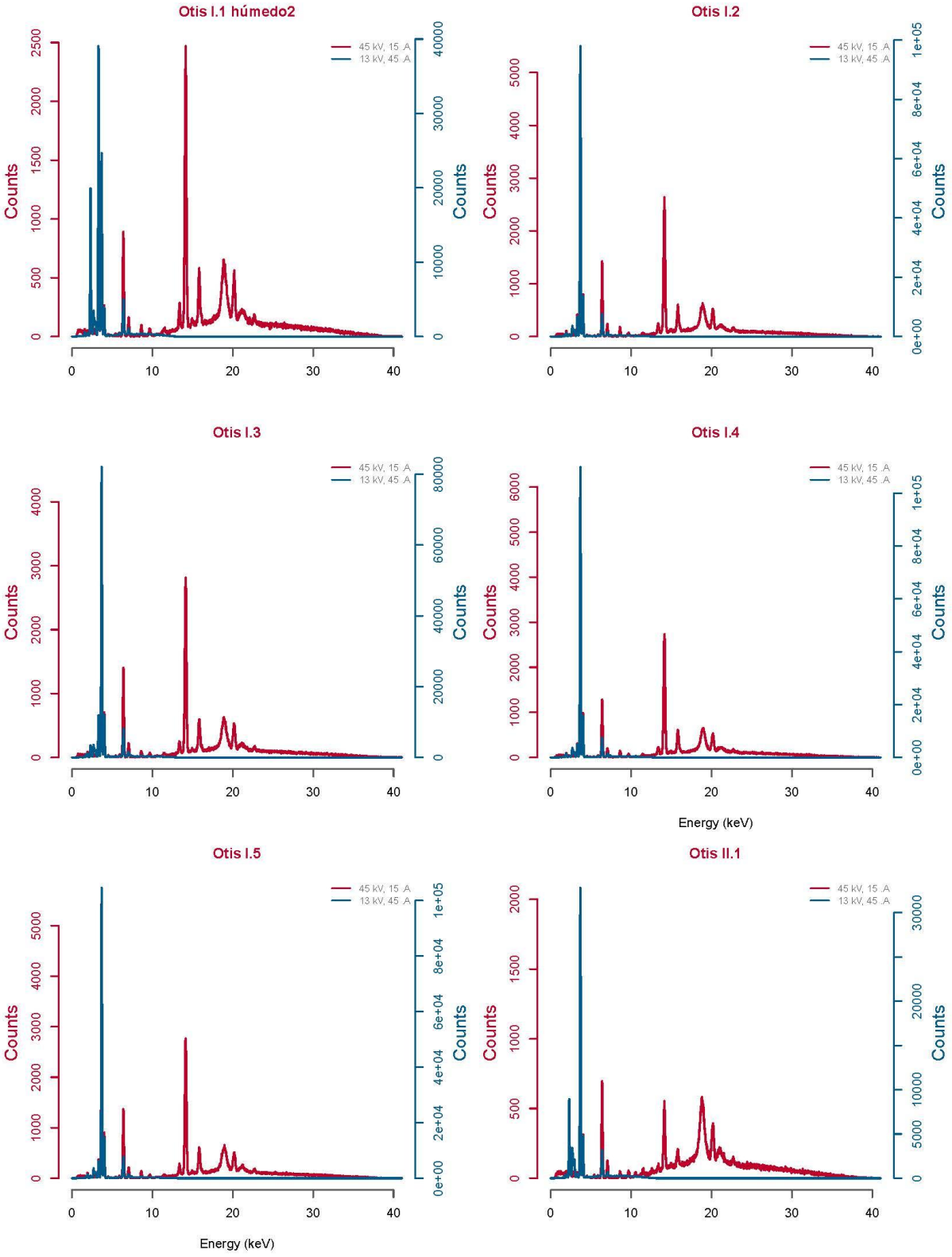
Otis I.1 húmedo2
Otis I.2
Otis I.3
Otis I.4
Otis I.5
Otis II.1
45 kV, 15 A
13 kV, 45 A
Counts
Energy (keV)

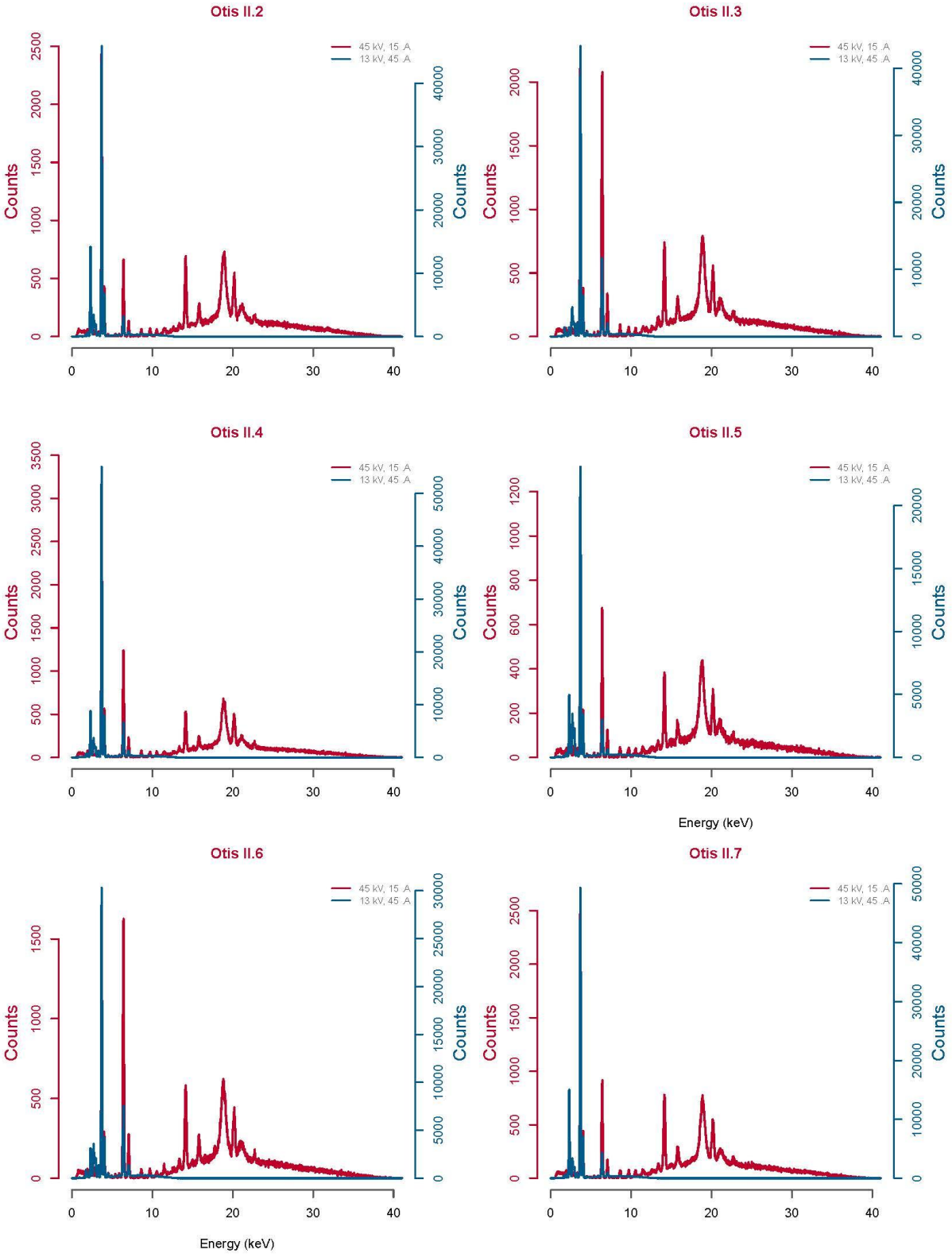
Otis II.2
Otis II.3
Otis II.4
Otis II.5
Otis II.6
Otis II.7
45 kV, 15 .A
13 kV, 45 .A
Counts
Energy (keV)

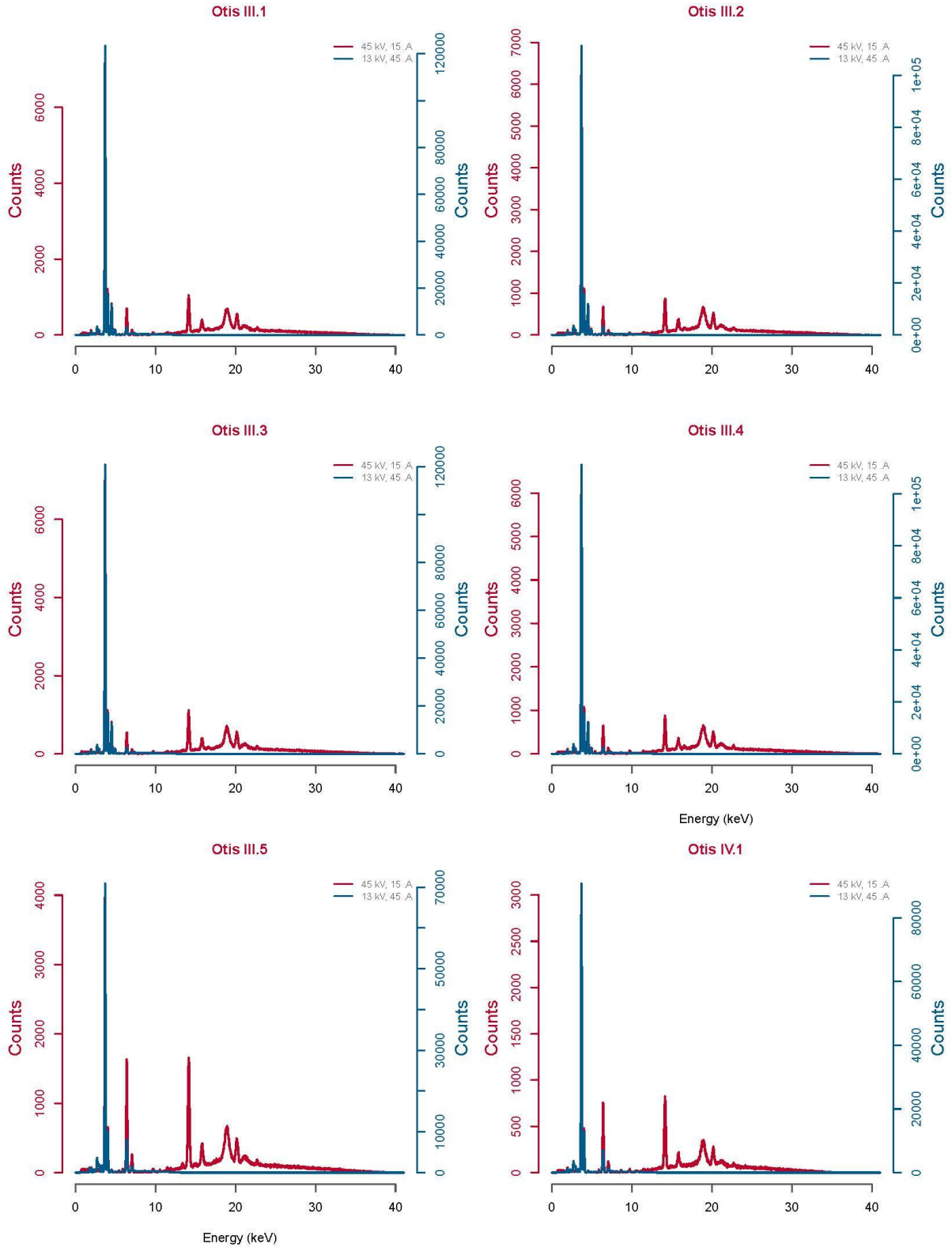

Figure 1-A. XRF spectra of the measurements done on the pilot site

Limits of detection for different types of Mining samples
X-MET7500 Mining Analyser

X-MET7500

Element	Mg	Al	P	S	K	Ca	Ti	V	Cr	Mn	Co	Ni
LOD (ppm)	3500	694	38	78	36	24	87	47	21	20	7	5

Element	Cu	Zn	As	Se	Sr	Zr	Nb	Mo	Rh	Ag	Cd	Sn
LOD (ppm)	4	4	1	1	2	4	4	3	13	11	18	20

Element	Sb	Ta	W	Au	Pt	Hg	Tl	Pb	Bi	U
LOD (ppm)	27	8	6	3	3	3	2	3	2	3

The limit of detection (LOD) is specified for a three sigma (99.7%) confidence level, and for a 2-condition method (2 x 60s).
All detection limits are specified for an interference-free matrix (SiO2 matrix).
Limits of detection effect the instrument precision (repeatability), but are not direct indication of the instrument accuracy.

Limits of detection are dependent on the following factors:
- Inter-elements effects (matrix interferences) and peaks overlaps
- Confidence level (number of sigma used to define the LOD)
- Analysis time

OXFORD INSTRUMENTS
The Business of Science®

Funded by the European Union

Limits of detection for different types of Soil samples
X-MET7500 Mining Analyser

X-MET7500

Element	K	Ca	Ti	V	Cr	Mn	Co	Ni	Cu	Zn	As	Se
LOD (ppm)	52	34	12	13	8	9	4	2	2	3	2	2

Element	Sr	Zr	Mo	Rh	Ag	Cd	Sn	Sb	Ba	Ta	W	Au
LOD (ppm)	3	2	3	10	8	9	14	15	74	6	6	3

Element	Hg	Tl	Pb	Th	U
LOD (ppm)	3	3	4	4	4

The limit of detection (LOD) is specified for a three sigma (99.7%) confidence level, and for a 2-condition method (2 x 60s).
All detection limits are specified for an interference-free matrix (SiO2 matrix).
Limits of detection effect the instrument precision (repeatability), but are not direct indication of the instrument accuracy.

Limits of detection are dependent on the following factors:
- Inter-elements effects (matrix interferences) and peaks overlaps
- Confidence level (number of sigma used to define the LOD)
- Analysis time

OXFORD INSTRUMENTS
The Business of Science®

Funded by the European Union

Elemental Detection Limits for different materials – Mining LE Package

X-MET7500

Elemental Detection limits on mining samples (SiO2 matrix), ppm

Meas time	Mg	Al	P	S	K	Ca	Ti	V	Cr	Mn	Co	Ni
60s+60s	5300	1000	120	100	15	15	106	58	34	22	9	6

Meas time	Cu	Zn	As	Se	Sr	Zr	Nb	Mo	Rh	Ag	Cd	Sn
60s+60s	4	3	3	3	3	6	6	5	20	16	2E	28

Meas time	Sb	Ta	W	Au	Pt	Hg	Tl	Pb	Bi	U
60s+60s	34	9	8	11	6	5	5	5	6	6

Limit of detection (LOD) is specified for each matrices in three sigma 99.7% confidence level. Individual LOD's improve as a function of the square root of the testing time. All detection limits are specified for interference free matrix.
LOD's are listed in parts per million (ppm). Limit of detection effects on instrument precision (repeatability), but it is not direct indication of instrument accuracy.

Limits of detection are dependent on the following factors.
- Matrix Interferences, overlapping elements etc.
- Level of statistical confidence
- Testing time

OXFORD INSTRUMENTS
The Business of Science®

SUM4Re

Funded by the European Union

Elemental Detection Limits for different materials –

Soil LE Package

X-MET7500

Elemental Detection limits on mining samples (SiO2matrix), ppm

Meas time	Mg	Al	P	S	K	Ca	Ti	V	Cr	Mn	Co	Ni	Cu	Zn	As	Se
60s+60s	5300	´000	120	100	15	15	106	58	34	22	9	6	4	3	3	3

Meas time	Sr	Zr	Mo	Rh	Ag	Cd	Sn	Sb	Ba	Ta	W	Au	Hg	Tl	Pb	Th	U
60s+60s	3	6	5	20	16	18	28	34	227	9	8	11	5	5	5	6	6

Limit of detection (LOD) is specified for each matrices in three sigma 99.7% confidence level. Individual LOD's improve as a function of the square root of the testing time. All detection limits are specified for interference free matrix.
LOD's are listed in parts per million (ppm). Limit of detection effects on instrument precision (repeatability), but it is not direct indication of instrument accuracy.

Limits of detection are dependent on the following factors.
- Matrix Interferences, overlapping elements etc.
- Level of statistical confidence
- Testing time

OXFORD INSTRUMENTS
The Business of Science®

SUM4Re

Funded by the European Union

Elemental Detection Limits for different materials – Restricted Materials

X-MET7500

Plastics

Elemental Detection limits on Polymers (Polyethylene plastic), ppm

Meas. Time	Cr	Br	Cd	Hg	Pb	Ni	Se	Sb	Ba	As	Cl
30s	9	< 5	12	1.2	1.0	6	< 5	24	124	< 5	0,92 %
60s	6	< 5	9	< 1	< 1	< 5	< 5	17	88	< 5	0,65 %
120s	<5	< 5	6	< 1	< 1	< 5	< 5	12	62	< 5	0,46 %

Metal Alloys

Elemental Detection limits in different Metal alloys, ppm

Matrix	Meas. Time	Cr	Cd	Pb
Al-matrix	30s	144	21	11
	60s	102	15	8
	120s	72	11	6
Cu-matrix	30s	52	30	55
	60s	37	21	39
	120s	26	15	28
Fe-matrix	30s	106	58	69
	60s	75	41	49
	120s	53	29	35
Sn-matrix	30s	513	65	38
	60s	363	46	27
	120s	257	33	19

Limit of detection (LOD) is specified for each matrices in three sigma 99.7% confidence level. Individual LOD's improve as a function of the square root of the testing time. All detection limits are specified for interference free matrix.
LOD's are listed in parts per million (ppm) unless otherwise stated.
Limit of detection effects on instrument precision (repeatability), but it is not direct indication of instrument accuracy.

Limits of detection are dependent on the following factors.
- -Matrix Interferences, overlapping elements etc.
- -Level of statistical confidence
- -Testing time

OXFORD INSTRUMENTS
The Business of Science®

SUM4Re

Funded by the European Union

Method	Meas. Time	Mg	Al	Si	S	P
Aluminium	30s	0,35	-	0,08	-	-
	60s	0,25	-	0,06	-	-
	120s	0,18	-	0,04	-	-
Copper LE	30s	-	0,47	0,14	0,14	0,06
	60s	-	0,33	0,10	0,10	0,04
	120s	-	0,23	0,07	0,07	0,03
Low alloy Steel LE	30s	-	-	0,18	0,03	0,06
	60s	-	-	0,13	0,02	0,04
	120s	-	-	0,09	0,01	0,03
Nickel LE	30s	-	0,55	0,17	-	-
	60s	-	0,39	0,12	-	-
	120s	-	0,28	0,08	-	-
Stainless LE	30s	-	-	0,20	0.03 - 0.07*	0.03 - 0.07*
	60s	-	-	0,14	0.02 - 0.05*	0.02 - 0.05*
	120s	-	-	0,10	0.01 - 0.04*	0.01 - 0.04*
Titanium LE	30s	-	0,38	-	-	-
	60s	-	0,27	-	-	-
	120s	-	0,19	-	-	-

* Depends on the Molybdenum content in the sample

Limit of detection (LOD) is specified for each matrices in three sigma 99.7% confidence level. Individual LOD's improve as a function of the square root of the testing time. All detection limits are specified for interference free matrix. LOD's are listed in wt%. Limit of detection effects on instrument precision (repeatability), but it is not direct indication of instrument accuracy.

Limits of detection are dependent on the following factors.
- Matrix Interferences, overlapping elements etc.
- Level of statistical confidence
- Testing time

Feb 2012

OXFORD INSTRUMENTS
The Business of Science®

Figure 2-A. Calibration data base of the p-XRF

SUM4Re

Creating materials banks
from digital urban mining

www.sum4re.eu sum4re@uvigo.gal SUM4Re SUM4Re_EU

Funded by the European Union. Views and opinions expressed are however those of the author(s) only and do not necessarily reflect those of the European Union. Neither the European Union nor the granting authority can be held responsible for them.

Funded by the European Union